

Attenuation caused by a Distant Isothermal Turbulent Screen

Jörg Fischer & Michael Dopita

Research School of Astronomy & Astrophysics, Institute of Advanced Studies, The Australian National University, Cotter Road, Weston Creek, ACT 2611 Australia

`fischer,mad@mso.anu.edu.au`

ABSTRACT

We analyse in detail the attenuation caused by an isothermal turbulent distant foreground dust screen. The attenuation curve is well determined by two parameters, the absolute-to-relative attenuation ratio $R_V^A = A_V/E(B - V)$ and the absolute attenuation A_V . We show quantitatively how these two observable quantities depend on the statistical properties of the local density and the mean attenuation $\langle A_V \rangle$ and how they vary with the thickness of the screen measured in units of the largest turbulent scale. The attenuation through a turbulent medium is characterised by higher transparency and a flatter attenuation curve in comparison with a homogeneous dust screen. In general, the effect of the turbulent medium on the attenuation increases with slice thickness. In the limit of thick slices, typically larger than the maximum turbulent scale, R_V^A asymptotically approaches a maximum value.

keywords ISM:dust—dust:extinction

1. Introduction

Dust grains in the interstellar medium attenuate the star light, in particular at UV wavelengths, and make it difficult to directly measure intrinsic parameters such as the star-formation rate of galaxies or to study highly obscured astrophysical objects like compact HII-regions. To quantify the star formation rate as a function of redshift z through UV-observations, a correction for attenuation is essential but is still very uncertain. One of the reasons is that the dust obscuration at high red-shift is not well understood, partly because of the lack of a satisfying physical model of the dust attenuation.

Due to its turbulent motion, most likely dominated by MHD-turbulence, the diffuse interstellar medium shows a very inhomogeneous fractal structure which has important consequences for the dust attenuation of star light from galaxies. This attenuation is qualitatively different to the extinction measured for single stars where the attenuation is simply

proportional to the column density and is caused by both absorption and scattering by dust grains.

By contrast the physics of the attenuation for the collected star light from galaxies is much more complex. It depends in general on the distribution of dust and gas, the variation of dust properties and the orientation of the galaxies with respect to the observer. A first approach, shown by Calzetti (2001) to be a very successful one, provides a model where all stars are seen through a foreground dust screen which can be assumed to be distant from stars. This is the model discussed in this paper.

In case of an inhomogeneous medium the extinction varies over the observed field. Regions of high column densities may be optically thick in the UV but optical thin in the IR while regions of low column densities may be optical thin over the whole wavelength range. Therefore, the effective extinction curve or attenuation curve for all stars seen through a turbulent dust screen is generally flatter than the extinction curve of single stars. Furthermore, since the light can escape efficiently through regions of low optical depth the attenuation of a turbulent screen is generally smaller than one would expect in case of an homogeneous ISM.

The flattening of the attenuation curve can be described by the absolute-to-relative attenuation ratio $R_V^A = A_V/E(B-V) = \tau_V/(\tau_B - \tau_V)$ which is determined by the effective optical depths τ_V and τ_B in V (0.548 μm) and B (0.44 μm). A flatter attenuation curve is characterised by a higher R_V^A . This value has to be distinguished from the R_V -value of pure extinction curves which is related to the extinction coefficients k_λ by $R_V = k_V/(k_B - k_V)$ and therefore can be used to infer some constraints on the dust properties. A larger R_V -value for example points to a larger grain population. In the limit of a homogenous distant screen both values are the same. In a turbulent medium the R_V^A will in general be larger than R_V of the underlying extinction curve.

Assuming that the dust properties have no spatial variation in the ISM, then the attenuation curve of the screen is determined by the probability distribution function (PDF) of the column density N alone. As found by Ostriker et al. (2001) using MHD-simulations the PDF of the column density of an isothermal medium should be approximately log-normal, the functional form also found for the PDF of the local density (Vázquez-Semadeni 1994; Padoan et al. 1997; Passot & Vázquez-Semadeni 1998).

Based on this hypothesis we have shown (Fischera et al. 2003) (Paper I) that the overall curvature of the attenuation curve, empirically derived for star-burst galaxies and known as the ‘Calzetti-extinction-curve’, can be naturally explained in terms of a turbulent dust screen. Below 2200 Å the empirical curve could be reproduced and the R_V^A -value was consistent with

the value of the ‘Calzetti-curve’. Furthermore, the lower values of the Mach-numbers derived from the fit was found to be in agreement with the Mach-numbers of our galaxies.

To obtain a deeper understanding of the attenuation caused by a turbulent foreground screen in Paper II we investigated how the PDF of the column density relates to the density distribution and the correlation function (the one point and the two point statistics) of the local density. We described how the standard deviation of the column densities varies with slice thickness and showed that for moderate log-normal density distributions of the local density ρ , where its standard deviation $\sigma_{\rho/\langle\rho\rangle}$ is not much larger than ~ 2.5 , the PDF can well be approximated by a log-normal density distribution. For $\sigma_{\rho/\langle\rho\rangle} > 1$ the approximation becomes less accurate, tending to systematically underestimate the probability of encountering high column densities and therefore tending to underestimate the standard deviation.

In this paper we will analyse in detail the attenuation curve caused by an isothermal turbulent dust screen using the analytical formula we derived in Paper II. We will describe how the attenuation curve depends on the statistical properties of the local density and how the attenuation curve varies with slice thickness.

2. Model of the turbulent dust screen

To analyse the attenuation caused by a distant turbulent screen we use an idealised model based on the one point and two point statistic as outlined in Fischer & Dopita (2004). The turbulent medium is taken to be isotropic and we assume that the power spectrum $P(\mathbf{k})=|\rho(\mathbf{k})|^2$ of the local density $\rho(\mathbf{r})$ is a simple power law $P(k) \propto k^n$ with power n where the scales extend from a minimum scale L_{\min} to a maximum scale L_{\max} . As in our previous paper we will consider a power spectrum with $n = -10/3$ and $n = -3$ which corresponds to Kolmogorov turbulence and to the isotropic MHD-model discussed by Iroshnikov (1964) and Kraichnan (1965), respectively. The turbulent medium is additionally described by the standard deviation $\sigma_{\rho/\langle\rho\rangle}$ of the local density, ρ , where $\langle\rho\rangle$ is its mean value.

In general the width of the density distribution increases as consequence of higher compression resulting from higher Mach numbers M . In particular for non-magnetised forced turbulence it has been found by using 3D-simulation (Padoan et al. 1997; Nordlund & Padoan 1999) that the standard deviation of the density is almost linearly correlated with Mach number:

$$\sigma_{\rho} \approx \beta M \langle \rho \rangle. \quad (1)$$

where $\beta \approx 0.5$. The more general case appears to be more complicated as for magnetised turbulence no simple correlation between density contrast and Mach number has been found.

However, as might be expected from the additional pressure support to the plasma provided by magnetic fields, it seems that the density contrast becomes weaker when magnetised turbulence is considered (Nordlund & Padoan 1999; Ostriker et al. 2001).

The actual standard deviation may change throughout the whole interstellar medium as the physical conditions vary. As shown in Paper I, the dispersion velocity of the cold neutral medium (CNM) and the warm neutral medium (WNM) of our galaxy suggests a Mach number of approximately 12 and 1.8, respectively. If the relation given in equation 1 is true the standard deviation should vary in the range ~ 0.9 to ~ 6 . More violent systems like star burst galaxies are likely to show higher Mach numbers. Their turbulent medium may therefore be characterised by a wider distribution of the local density.

The standard deviation $\sigma_{N/\langle N \rangle}$ of the normalised column density N is determined by the thickness Δ/L_{\max} of the turbulent screen and the power spectrum of the local density. For simplicity we assume that the PDF of the column density N through a turbulent isothermal medium is described by a simple log-normal density distribution and therefore by the same functional form as the PDF of the local density. The PDF of the normalised column density $\xi = N/\langle N \rangle$ is then described by

$$p(\ln \xi) = \frac{1}{\sqrt{2\pi}\sigma_{\ln N}} e^{-x^2/2\sigma_{\ln N}^2} \quad (2)$$

with $x = \ln \xi - \ln \xi_0$ where $\ln \xi_0 = -\frac{1}{2}\sigma_{\ln N}^2$. The standard deviation $\sigma_{\ln N}$ of the log-normal density distribution is connected with the standard deviation $\sigma_{N/\langle N \rangle}$ by:

$$\sigma_{N/\langle N \rangle}^2 = e^{\sigma_{\ln N}^2} - 1. \quad (3)$$

For small fluctuations of the local density up to $\sigma_{\rho/\langle \rho \rangle} = 1$ the assumption of a log-normal PDF seems to be very accurate. If the medium is more turbulent the PDF of the column density may show some deviations from the log-normal distribution even though the overall shape seems to be well preserved. We will discuss the consequences of this in Sect. 5.1.1.

As in Paper I we assume that the dust properties are not varying throughout the whole turbulent density structure so that the optical depth is simply given by $\tau_\lambda = Nk_\lambda$ where k_λ is the wavelength dependent extinction coefficient. The underlying extinction curve is assumed to be the mean extinction curve of our galaxy where we adopted the curve obtained by Weingartner & Draine (2001). As this curve has been derived by fitting a dust model to the mean extinction curve it also provides further information about the scattering properties. As this paper describes the attenuation of a distant dust screen, dust scattered light does not contribute to the measured light.

The main parameter determining the attenuation of a distant turbulent dust screen is the PDF of the optical depths. Due to the log-normal density distribution the light of an extended source or a distribution of stars behind the screen can suffer a large point-to-point variation of extinction, $e^{-\tau}$. The amplitude of this variation will depend on the strength of the fluctuation of the column densities. On average the turbulent screen leads to an effective extinction τ_{eff} given by:

$$\tau_{\text{eff}} = -\ln \left(\int d \ln(\xi) p(\ln(\xi)) e^{-\xi \langle \tau \rangle} \right) \quad (4)$$

$$= -\ln \left(\int dy p(y) e^{-e^y \langle \tau \rangle} \right), \quad (5)$$

where $e^y = \xi = \tau / \langle \tau \rangle$.

In Fig. 1 the attenuation caused by a turbulent dust screen is visualised as function of mean optical depth $\langle \tau \rangle$ and standard deviation $\sigma_{\ln N}$ of the log-normal density distribution. By increasing $\sigma_{\rho/\langle \rho \rangle}$ the column density in certain areas is enhanced while the regions in between becomes almost free of material. The effect of the column density fluctuation on extinction increases both with $\sigma_{\rho/\langle \rho \rangle}$ and with mean optical depth of the screen. While the screen with $\sigma_{\rho/\langle \rho \rangle} = 0.25$ seems to be rather uniform, for higher values of $\sigma_{\rho/\langle \rho \rangle}$ extinction at certain areas becomes rather high. These regions appear as dark clouds. As the regions of low optical depth transmit light very efficiently, the transmission of a turbulent screen, or general of all clumpy media, is higher than in the case of a homogeneous medium. Therefore, for the same mean optical depth the effective extinction decreases with $\sigma_{\rho/\langle \rho \rangle}$.

If we compare the transmission for different mean optical depths but the same fluctuations of column densities then the structure appears more clearly towards higher values of $\langle \tau \rangle$. This reflects the fact that the difference of the extinction of regions with different optical depth increases. This can be easily seen if two regions with optical depths τ_1 and τ_2 with $\tau_2 > \tau_1$ are considered where the ratio in extinction is $e^{\tau_2 - \tau_1}$. If we scale the mean optical depth by a factor f then the ratio becomes $e^{f(\tau_2 - \tau_1)}$. As consequence the contrast between high transmission regions and low transmission regions in a turbulent screen becomes larger for higher values of the mean optical depth. If we consider the effective extinction as function of wavelength then a flattening of the curve is expected either when the mean optical depth or when the fluctuations of the column density increases.

In this paper we will quantitatively analyse these effects of the turbulent dust screen on the attenuation curve. In Sect. 3 we will discuss attenuation curves as function of the standard deviation $\sigma_{\ln \tau}$ and the mean attenuation $\langle A_V \rangle = 2.5 \log_{10} e^1 \langle \tau_V \rangle$ of the turbulent dust screen. We will show how these physical quantities relate to the observed quantities, the absolute-to-relative attenuation ratio $R_V^A = A_V / E(B - V)$ and the attenuation A_V . In

Sect. 4.1 and Sect. 4.2 we describe how A_V and R_V^A vary with slice thickness Δ/L_{\max} and mean attenuation $\langle A_V \rangle$ and how the attenuation curves are effected by the statistical properties (the standard deviation $\sigma_{\rho/\langle \rho \rangle}$ and the power spectrum $P(k)$) of the local density. Finally, we discuss which conclusions can be made about the turbulent density structure by measuring the attenuation curve.

3. Attenuation of a distant turbulent screen

In Fig. 2 the observable quantities A_V and R_V^A are shown in the physical plane defined by the standard deviation $\sigma_{A_V/\langle A_V \rangle} = \sigma_{\tau/\langle \tau \rangle}$ of the fluctuation of optical depths and the mean attenuation $\langle A_V \rangle$. In the limit of both small attenuation $\langle A_V \rangle$ and small fluctuations the attenuation approaches the limit of the homogeneous dust screen where $R_V^A = R_V = 3.08$.

As expected the attenuation curve becomes flatter by increasing either the optical depth or the fluctuations of the optical depth. This results in higher values of R_V^A . In the limit of small fluctuations, as will be verified in Sect. 3.2, the contours of constant R_V^A -values are described by $\sigma_{\ln \tau}^2 \langle \tau \rangle = \text{constant}$. The same lines also have $A_V / \langle A_V \rangle = \text{constant}$.

The curves with $R_V^A = \text{const.}$ describe essentially identical attenuation curves A_λ/A_V . This is particularly true when the relation $A_\lambda / \langle A_\lambda \rangle = \text{const.}$ is valid over the whole wavelength range.

The maximum flattening that can be produced by the turbulent screen is determined by the physical conditions. If we consider the Mach numbers in the ISM of our galaxy the standard deviation of the column density should be smaller than 10. In case of an attenuation $A_V = 1$ we would expect attenuation curves with R_V^A -values smaller than 10. The flattening produced in more optical thick systems can be much more pronounced.

Naively one would expect that in the limit of small fluctuations of the optical depth the attenuation can be described by a homogeneous screen. But as the flattening is a function of $\sigma_{\ln \tau}^2 \langle \tau \rangle$ a screen with very small fluctuations can effectively produce the same attenuation curve as a screen with strong fluctuations. The mean optical depths however is very different.

In Fig. 3 and Fig. 4 we show the variation of the attenuation curves as a function of R_V^A . In Fig. 3 they are given as a function of the relative attenuation

$$\mathcal{E}_\lambda = \frac{A_\lambda - A_V}{A_B - A_V} = \frac{E(\lambda - V)}{E(B - V)}. \quad (6)$$

The attenuation A_V is held fixed with $A_V = 1$ and $A_V = 100$, respectively. The curves obtained for the same R_V^A -value for the two choices of the attenuation A_V are essentially the

same even though they imply very different physical conditions of the turbulent screen. In the case of $A_V = 1$ an R_V^A -value of 10 would correspond to a screen with strong fluctuations of the optical depth with $\sigma_{\tau/\langle\tau\rangle} \approx 50$. For $A_V = 100$ the fluctuations would be very small with $\sigma_{\tau/\langle\tau\rangle}$ less than ≈ 0.4 .

As can be seen in the figure the curvature itself allows a determination of the R_V^A -value. The curves are compared with the curve empirically derived for star-burst galaxies, known as the ‘Calzetti-extinction-law’. At wavelengths below the extinction bump at 2200 Å the ‘Calzetti-curve’ is obtained for $R_V^A \approx 4.3$. As is shown below, in reality variations of R_V^A are expected by comparing the attenuation of different galaxies. In star-burst galaxies the bump at 2200 Å seems to be absent. As we show elsewhere (Dopita et al. 2005) this can be understood if the carriers of the 2200 Å absorption feature are the PAH molecules, which are photo-dissociated in the strong EUV radiation field of these galaxies.

In Table 1 the attenuation \mathcal{E}_λ of an isothermal turbulent dust screen is given for several values of R_V^A . The attenuation in V is taken to be $A_V = 1$ and $A_V = 10$, respectively. The attenuation A_λ can be obtained by using the following formula:

$$A_\lambda = (\mathcal{E}_\lambda / R_V^A + 1) A_V. \quad (7)$$

3.1. General attenuation curve

In the previous section we discussed the effect of the turbulent screen on the attenuation curve using the mean extinction curve of our galaxy. But in general the underlying extinction curve of a turbulent screen might not be the same. The extinction curve might show a different wavelength dependence and might be characterised by another R_V -value. It is therefore appropriate to use a more general approach where these effects can be easily taken into account.

For this we considered the attenuation A_λ/A_V of the turbulent screen as function of $x = \langle A_\lambda \rangle / \langle A_V \rangle = k_\lambda/k_V$ rather than as function of wavelength. To characterise the attenuation curves we used the absolute-to-relative attenuation ratio $\alpha_V^A = A_V/E(\tilde{\lambda} - V)$ where the wavelength $\tilde{\lambda}$ is defined by the absolute-to-relative extinction $\alpha_V = k_V/(k_{\tilde{\lambda}} - k_V) = 3.08$. The variation of α_V^A is therefore taken to be identical to the variation of R_V^A of the mean extinction curve of our galaxy.

We considered the ratio of the extinction coefficients k_λ/k_V in the range 0.1 to 10. As shown in the previous sections the attenuation is well determined by the α_V^A -value, largely independent of the actual conditions, the mean attenuation $\langle A_V \rangle$ and the contrast $\sigma_{\tau_V/\langle\tau_V\rangle}$. The dependence on the absolute attenuation A_V , on the other hand, is only weak. To obtain

a general expression for the attenuation curve we hold the absolute attenuation A_V constant and considered all attenuation curves up to $\alpha_V^A = 10$. The absolute attenuation A_V has been chosen to be 1 and 10. The derived attenuation curves, shown in Fig. 5 for $A_V = 10$, can be fitted by a simple polynomial function

$$\log A_\lambda/A_V = \sum_{i=1}^3 a_i (\log x)^i \quad (8)$$

where the constants a_i depend on the absolute-to-relative attenuation ratio α_V^A . The accuracy of all fitted curves obtained for $A_V = 1$ and $A_V = 10$ is better than 0.55% and 0.65%, respectively. The variation of the parameter a_i as function of α_V^A are shown in Fig. 6.

We performed an individual polynomial fit to the coefficients with

$$a_i(z) = \sum_{j=0}^{N_i} b_j z^j \quad (9)$$

where $z = 1/(\alpha_V^A - 1)$ and $N_1 = 3$ and $N_2 = N_3 = 4$. The result is also shown in Fig. 6. The fitted coefficients b_j are given in Table 2.

If applied to situations where the absolute attenuation A_V is either 1 or 10, the approximations are better than 1.3%. In general the accuracy is somewhat lower. If the approximation obtained for $A_V = 1$ is used for a turbulent medium where $A_V = 10$ the accuracy is better than $\sim 5\%$. The largest errors occurs at low optical depths. For $x \geq 1$ the approximation is better than $\sim 2\%$.

3.1.1. Attenuation curves for different R_V

The approximations above can be directly applied for extinction curves with an absolute-to-relative extinction $R_V \approx \alpha_V = 3.08$. For extinction curves with a different R_V one can use a simple linear transformation. The correct attenuation curve for a given R_V^A is obtained by applying the relation

$$\alpha_V^A = \frac{1}{m} (R_V^A - R_V) + \alpha_V \quad (10)$$

where m is a linear function of R_V with

$$m = 1 + 0.275 (R_V - \alpha_V). \quad (11)$$

The simple correction has been obtained by varying R_V from 2 to 6 and by using the approximation for $A_V = 1$ and $A_V = 10$. For the considered parameter range of R_V and α_V^A the accuracy of the approximation is better than $\sim 0.6\%$.

3.2. Analytical approximation of τ_{eff}

In the limit of an optical thick slice with $\langle \tau \rangle \gg 1$ and in the limit of small fluctuations of the optical depth with $\sigma_{\tau/\langle \tau \rangle} \ll 1$ an analytical expression for the effective optical depth can be given. This approximation is particularly useful in deriving the attenuation of thick slices of the turbulent medium.

The function $e^{-e^y \langle \tau \rangle}$ stays almost constantly 1 for $y < -\ln \langle \tau \rangle$ and drops sharply at larger values. In the limit $\ln \langle \tau \rangle \ll y_0$ the function $p(y) e^{-e^y \langle \tau \rangle}$ becomes a narrow distribution around a maximum at \tilde{y} . By using the approximation

$$e^y \approx e^{\tilde{y}} (1 + (y - \tilde{y}) + \frac{1}{2}(y - \tilde{y})^2) \quad (12)$$

it is straight forward to show that the effective extinction is given by

$$\tau_{\text{eff}} = \frac{1}{2} \ln \gamma + \frac{1}{2} \langle \tau \rangle e^{\tilde{y}} (1 + \gamma) \quad (13)$$

where $\gamma = 1 + \langle \tau \rangle \sigma_{\ln \tau}^2 e^{\tilde{y}}$ and where \tilde{y} is the solution of the equation:

$$\tilde{y} - y_0 = -\sigma_{\ln \tau}^2 \langle \tau \rangle e^{\tilde{y}} \quad (14)$$

In the limit of small fluctuations of the optical thickness and $\langle \tau \rangle \ll 1$ the maximum is at $\tilde{y} \approx y_0 = -\frac{1}{2} \sigma_{\ln \tau}^2 \ll 1$ so that $\gamma \approx 1$. Therefore, the approximation is still valid and gives the correct result $\tau_{\text{eff}} \approx \langle \tau \rangle$.

In Fig. 7 we compare the effective optical depth obtained by solving the integral 4 and by using the approximation 13. As shown the analytical solution is accurate for small fluctuations for all optical depths and can be used at higher optical depths also for larger fluctuations. In case of an effective optical depth $\tau_{\text{eff}} = 1$ the uncertainty by using the approximation is at most 1%.

If only small fluctuations of the optical depths are considered the first part of the approximation 13 can be neglected. Furthermore $y_0 = \frac{1}{2} \sigma_{\ln \tau}^2 \approx 0$ in Eq. 14 so that τ_{eff} becomes a function of the product $\sigma_{\ln \tau}^2 \langle \tau \rangle$ only.

In the limit $\sigma_{\ln \tau} \ll 1$ the attenuation is given by

$$A_\lambda = \frac{1}{2} \langle A_\lambda \rangle e^{\tilde{y}_\lambda} (1 - \frac{1}{2} \tilde{y}_\lambda) \quad (15)$$

so that $A_\lambda / \langle A_\lambda \rangle = \text{constant}$ for $\sigma_{\ln \tau}^2 \langle \tau \rangle = \text{constant}$.

In addition the absolute-to-relative attenuation ratio R_V^A in the limit of small fluctuations of the optical thickness becomes only a function of $\sigma_{\ln \tau}^2 \langle \tau \rangle$ and is given by the expression

$$R_V^A = \frac{A_V}{A_B - A_V} = \frac{\tilde{y}_V(2 + \tilde{y}_V)}{\tilde{y}_B(2 + \tilde{y}_B) - \tilde{y}_V(2 + \tilde{y}_V)}. \quad (16)$$

As the width of the PDF of the column density decreases with thickness and the fluctuations will therefore always be small at a certain point both approximations are in particular helpful to describe the attenuation caused by dust screens which are larger than the maximum scale L_{\max} . We will discuss this in Sect. 4.5.

4. Attenuation with slice thickness

In the following we analyse in some detail how the attenuation curve depends on the statistical properties of the local density of the turbulent density structure and how the attenuation curve is varying with the thickness of the distant screen where we consider the ratio Δ/L_{\max} of its thickness Δ and the maximum turbulent scale L_{\max} . The effects on the attenuation curves are discussed by considering R_V^A and $\langle A_V \rangle$ as these parameters determine the attenuation sufficiently well. The attenuation through the turbulent medium is furthermore characterised by the mean optical depth $\langle \tau \rangle_{L_{\max}}$ or the corresponding attenuation $\langle A_V \rangle_{L_{\max}}$ at one maximum turbulent scale L_{\max} .

4.1. Variation of A_λ with slice thickness

A very thin slice through the turbulent density structure is obviously also optically thin. In this case $\langle A_\lambda \rangle = A_\lambda$. By increasing the thickness, some parts start to become optically thick and the effective extinction or the attenuation becomes smaller than the value of an homogeneous screen. To visualise the effect we considered the corresponding attenuation at a thickness of one maximum scale L_{\max} . The variation of $A_\lambda/(\Delta/L_{\max})$ with slice thickness for different assumptions of the mean attenuation $\langle A_\lambda \rangle_{L_{\max}}$ is shown in Fig. 8. The standard deviation $\sigma_{\rho/\langle \rho \rangle}$ of the local density is considered to be 1.0, 5.0, and 10.0. For Kolmogorov turbulence we have chosen $\zeta = L_{\max}/L_{\min} = 10^5$ high enough to have an effect on the results. For a turbulent medium with $n = -3$ we have chosen a scaling relation ranging over 10 magnitudes.

As expected the effect of the turbulent screen increases with $\sigma_{\rho/\langle \rho \rangle}$ and $\langle A_\lambda \rangle_{L_{\max}}$. In case of slices thinner than the maximum scale the attenuation $A_\lambda/(\Delta/L_{\max})$ drops relatively strongly with slice thickness. In the limit of slices typically larger than the maximum scale the attenuation approaches asymptotically a lower limit. As will be shown, this limit is, for a given power spectrum, determined by the single expression $\sigma_{\rho/\langle \rho \rangle}^2 \langle \tau \rangle_{L_{\max}}$. The screen will be significantly different from the homogeneous screen if this expression is larger than ~ 1 independent of the actual fluctuations of the column density.

The effect of a turbulent medium on the attenuation is weaker in case of a power spectrum with $n = -3$. This is expected as there is more power in small density fluctuations. Due to averaging effects the standard deviation $\sigma_{N/\langle N \rangle}$ of such a medium is smaller than the corresponding value of a Kolmogorov turbulent medium (see Paper II).

4.2. Variation of R_V^A with slice thickness

To study the effect of the slice thickness of the screen on R_V^A we considered the same turbulent density structures as in Sect. 4.1. The variation of R_V^A with slice thickness is shown in Fig. 9.

The dependence of R_V^A with slice thickness reflects the behaviour of A_V . In general the attenuation curves become flatter with increasing thickness of the dust screen. The R_V^A -value increases strongly with slice thickness if the slice is thin in comparison with the largest scale L_{\max} but approaches a maximum value for thick slices once the thickness is larger than L_{\max} . The flattening is stronger in more turbulent media characterised by a larger standard deviation $\sigma_{\rho/\langle \rho \rangle}$ and in more optical thick media. As expected from the results found for A_V the flattening is much weaker in the case of $n = -3$.

4.3. R_V^A as function of A_V

In Fig. 10 we show how the relation of the two observable quantities R_V^A and A_V is affected by different conditions of the turbulent medium. As can be seen in the figure, for given attenuation A_V the attenuation curve flattens for higher values of the mean attenuation $\langle A_V \rangle_{L_{\max}}$. The flattening as function of A_V for given $\langle A_V \rangle_{L_{\max}}$ is strongest in a region where $A_V < 1$.

One has to be aware that the R_V^A -value for a certain attenuation A_V depends on the slice thickness. As an example we can consider a turbulent medium with standard deviation $\sigma_{\rho/\langle \rho \rangle} = 1$ and $n = -10/3$. If $A_V = 1$ then $R_V^A < 3.3$ unless the thickness is smaller than $\Delta/L_{\max} = 1$.

The relation shown in Fig. 10 has consequences for the interpretation of the change by dust obscuration of the intrinsic spectral energy distribution from galaxies. A stellar spectrum well described over a certain wavelength range by a simple power law $I_\lambda \propto \lambda^\beta$ (Calzetti et al. 1994) with power β will have a different functional form if seen through a dust screen. If the spectrum is observed at two different wavelengths λ_1 and λ_2 the inferred

power $\tilde{\beta}$ would be different from β by

$$\begin{aligned}\Delta\beta &= \beta - \tilde{\beta} = \frac{\tau_{\lambda_1} - \tau_{\lambda_2}}{\ln \lambda_1 - \ln \lambda_2} \\ &= \frac{1}{\tilde{R}_{\lambda_2}^A} \frac{\tau_{\lambda_2}}{\ln \lambda_1 - \ln \lambda_2}.\end{aligned}\quad (17)$$

Here, we introduced the absolute-to-relative attenuation ratio $\tilde{R}_{\lambda_2}^A = \tau_{\lambda_2}/(\tau_{\lambda_1} - \tau_{\lambda_2})$. τ_{λ_1} and τ_{λ_2} are the effective optical depths at wavelength λ_1 and λ_2 .

As can be seen in Fig. 10 the variation $\Delta\beta$ depends linearly on the optical depth only in the limit of a thick slice with $\Delta/L_{\max} \gg 1$ or in case of a homogeneous screen where $\tilde{R}_{\lambda_1}^A = \tilde{R}_{\lambda_1}$ and is determined by the extinction coefficients k_{λ_1} and k_{λ_2} . In case of a turbulent screen the attenuation curve is more flat and therefore $\Delta\beta$ smaller in comparison with a homogeneous screen with the same attenuation A_V .

4.4. Attenuation for certain thickness

In Fig. 11 we show both the attenuation A_V and the absolute-to-relative attenuation ratio R_V^A in the parameter plane defined by $\sigma_{\rho/\langle\rho\rangle}$ and $\langle A_V \rangle$ for three slices through the turbulent density structure with varied thickness Δ/L_{\max} chosen to be 0.1, 1.0, and 10.0. The plot is similar to the one shown in Fig. 2 where the attenuation is shown as function of $\sigma_{\tau/\langle\tau\rangle}$ and $\langle A_V \rangle$.

The lines of constant R_V^A are defined by $\sigma_{\rho/\langle\rho\rangle}^2 \langle\tau\rangle = \text{constant}$ in the region where they become parallel. In this region constant R_V^A also defines $A_V/\langle A_V \rangle = \text{constant}$. As is shown in Sect. 4.5 this characteristic behaviour appears in the limit of thick slices with $\Delta/L_{\max} \gg 1$ and where $\sigma_{\ln\tau} \ll 1$.

4.5. Approximation for thick slices

In the limit of thick slices with $\Delta/L_{\max} \gg 1$ the effect of a turbulent screen on the attenuation curve can be described analytically for the case where the fluctuations of the optical depths become sufficiently small. As discussed in Paper II the standard deviation of the column density of a thick slice through the turbulent medium with standard deviation $\sigma_{\rho/\langle\rho\rangle}$ and a power spectrum with $n \neq -3$ and $n \neq -2$ is given by

$$\sigma_{N/\langle N \rangle}^2 = \frac{1}{2} \sigma_{\rho/\langle\rho\rangle}^2 \frac{(n+3)(1-\zeta^{n+2})}{(n+2)(1-\zeta^{n+3})} \left(\frac{\Delta}{L_{\max}} \right)^{-1} \quad (18)$$

and for $n = -3$ by

$$\sigma_{N/\langle N \rangle}^2 = \sigma_{\rho/\langle \rho \rangle}^2 \frac{1 - 1/\zeta}{2 \ln \zeta} \left(\frac{\Delta}{L_{\max}} \right)^{-1}. \quad (19)$$

If $\sigma_{\ln N} \ll 1$ then Eq. 3 can be replaced by $\sigma_{\ln N} \approx \sigma_{N/\langle N \rangle}$. Therefore, the product $\sigma_{\ln N}^2 \langle \tau \rangle$ becomes a constant. For a power spectrum with $n < -3$ and $\zeta \gg 1$ this expression is given by:

$$\sigma_{\ln N}^2 \langle \tau \rangle = \frac{1}{2} \frac{n+3}{n+2} \sigma_{\rho/\langle \rho \rangle}^2 \langle \tau \rangle_{L_{\max}} \quad (20)$$

and for $n = -3$ and $\zeta \gg 1$ by

$$\sigma_{\ln N}^2 \langle \tau \rangle = \frac{1}{2} \frac{1}{\ln \zeta} \sigma_{\rho/\langle \rho \rangle}^2 \langle \tau \rangle_{L_{\max}} \quad (21)$$

where $\langle \tau \rangle_{L_{\max}}$ is the mean optical depth for a slice with thickness $\Delta = L_{\max}$. In the limit of a thick slice the attenuation $A_\lambda / \langle A_\lambda \rangle$ and the absolute-to-relative attenuation ratio R_V^A become simply a function of the product $\sigma_{\rho/\langle \rho \rangle}^2 \langle \tau_\lambda \rangle_{L_{\max}}$ and can be derived by using the approximations of equations 15 and 16.

The dependence of $A_\lambda / \langle A_\lambda \rangle$ and R_V^A on $\sigma_{\rho/\langle \rho \rangle}^2 \langle \tau_\lambda \rangle_{L_{\max}}$ in the limit of thick slices is shown in Fig. 12. The power n is chosen to be $-11/3$, $-10/3$, and -3 . For all cases a scaling relation extending over 10 magnitudes is assumed.

The effect of the turbulent dust screen increases towards steeper power laws. For $n = -10/3$ or $n = -11/3$ the attenuation starts to deviate significantly from the homogeneous screen for $\sigma_{\rho/\langle \rho \rangle}^2 \langle \tau \rangle_{L_{\max}} \approx 1$. In case of flatter power laws the transition from a homogeneous to a clumpy screen is shifted towards higher values.

For a known power spectrum the combined information of R_V^A and A_V allows a determination of $\langle A_V \rangle$. If these curves are applied in cases of turbulent screens which are not necessarily thick the derived value has to be considered as *lower limit*.

In Fig. 13 the attenuation caused by a thick turbulent screen is shown in the plane defined by $\sigma_{\rho/\langle \rho \rangle}$ and $\langle A_V \rangle / (\Delta / L_{\max})$. As seen all contour lines defining different attenuation curves (or R_V^A -values) are now parallel. The curves showing different values of the attenuation $A_V / (\Delta / L_{\max})$ can be obtained by shifting a single curve along those parallel lines.

5. Discussion

5.1. Accuracy of the model

5.1.1. Error caused by the representation of the PDF by a log-normal density function

The largest uncertainty in the calculations as presented here is caused by the simplification of the PDF of the column densities by a log-normal density distribution. As we have shown in Paper II, deviations exist when turbulent density structures with $\sigma_{\rho/\langle\rho\rangle} > 1$ are considered and these deviations become more prominent for a wider PDF of the local density. Therefore, the correlation between the standard deviation $\sigma_{N/\langle N \rangle}$ and the standard deviation $\sigma_{\ln N}$ of the log-normal density distribution as given in Eq. 3 is not strictly valid in case of broad distributions of the local density. By using this correlation, we might overestimate the probabilities at low column densities but underestimate those at high column densities.

As the attenuation is mainly determined by the probabilities of low optical depths a better result would be obtained by using a log-normal density distribution with smaller standard deviation. This is particularly true in the case of turbulent media with high mean optical depth.

As stated in Paper II that the difference between the actual PDF and the log-normal density distribution becomes smaller for thick slices and should disappear altogether in the limit of slices with a thickness much larger than the maximum scale L_{\max} . In this case the PDF becomes a narrow Gaussian centred around unity. Therefore, the results presented for very thick slices will be accurate. The same applies for very thin slices where the PDF of the column density is very similar to the PDF of local density.

The largest difference will appear for slices slightly larger than one maximum scale and for wide density distributions of the local density. As the PDF overestimates the probabilities at low column densities the effect caused by the turbulent screen would be smaller than presented here. The actual transparency would be lower and the R_V^A -value smaller.

To assign an uncertainty to the data presented here we simply assume that the actual form is still represented by a log-normal density distribution but with a smaller standard deviation $\sigma_{N/\langle N \rangle} = \sigma_{A_V/\langle A_V \rangle}$. The derived uncertainties of the quantities A_V and R_V^A is shown in Fig. 14. As can be seen the effect due to uncertainties in the standard deviation depends on the mean attenuation $\langle A_V \rangle$ and the standard deviation of the column density. The error of the attenuation increases generally with optical thickness and can be quite substantial in case of turbulent media with very high mean optical depth. The accuracy of R_V^A is somewhat smaller.

In Paper II we analysed the uncertainty by approximating the PDF of the column density by a simple log-normal density distribution. The results can not be simply generalised as they may depend on the dynamic range of the turbulent density structure which in these calculation was only $\zeta = 5.4$. However, for a standard deviation of $\sigma_{\rho/\langle\rho\rangle} = 2.5$ the maximal error of the standard deviation of the column density was found to be slightly larger than 12% which appears at a slice thickness of $\Delta/L_{\max} \approx 2$. Assuming a linear increase of the error then the maximal error for $\sigma_{\rho/\langle\rho\rangle} = 5$ is roughly 25% and the maximal error for $\sigma_{\rho/\langle\rho\rangle} = 10$ already $\sim 50\%$.

But even for these extreme turbulent media with broad density distributions of the local density the R_V^A -values derived here will have less than $\sim 10\%$ error if the screen has a mean attenuation $\langle A_V \rangle = 1$. For a screen with ten times higher mean attenuation the accuracy is still better than $\sim 15\%$.

5.1.2. Dependence on ζ

In general the attenuation with slice thickness depends not only on the number of turbulent scale length but also on the dynamic range ζ of the turbulent density structure. For comparison we calculated the attenuation A_V and R_V^A as function of slice thickness assuming a relatively low value $\zeta = 10$. The standard deviation of the local density is chosen to be $\sigma_{\rho/\langle\rho\rangle} = 5$. The results are shown in Fig. 15 and Fig. 16. If the turbulence extends over a smaller dynamic range, then the averaging effect along the line of sight is smaller, and the distribution of the column densities is therefore wider. As consequence the screen will be more transparent and the flattening of the attenuation curve greater, or its R_V^A -value larger.

As seen in the figure the effect for Kolmogorov turbulence is relatively small but for $n = -3$ the differences are quite substantial. In fact the results obtained for both different assumptions of the scaling relation are now quite similar as the standard deviation of the column density is now almost identical, as can be seen in Fig. 3 in Paper II.

Simulations are necessarily quite limited and are not able to reproduce a scaling relation over several magnitudes as measured for the ISM. As mentioned already in Paper II the accuracy of the attenuation derived by using simulations and the conclusion about the statistical properties of the medium will depend on the actual power law of the turbulent density structure. For $n < -3$ the error might be quite small as in case of Kolmogorov turbulence but for $n \geq -3$ this effect will obviously be important.

5.2. Application of the model

Despite the simplicity of the model presented here, which does not take into account scattered light, it may well prove useful in helping to understand the attenuation of the light from highly obscured objects such as young compact HII-regions or even of entire galaxies. As the model is based on the physical properties of the turbulent density structure it may lead to realistic corrections which will be helpful to determine intrinsic important parameters as such as emission line ratios or star-formation rates. As discussed in Paper I the model already has been proven to be a natural explanation of the attenuation curve (the ‘Calzetti-extinction-law’) derived empirically for star burst galaxies.

The model connects the observable quantities A_V and R_V^A with the physical parameters $\sigma_{\rho/\langle\rho\rangle}$, $\tau_{L_{\max}}$, and Δ/L_{\max} and provides therefore a method to provide insight into the turbulent density structure through measurement of the attenuation curve alone. A major complication in the interpretation is certainly the fact that the turbulent medium is characterised by three parameters (for known power spectrum) while the attenuation curve only provides two.

A conservative lower limit of the standard deviation of the local density can be obtained by considering a turbulent screen with a thickness much larger than the maximum scale L_{\max} . A better estimate of the turbulence can be achieved by analysing the variation of the attenuation curve with slice thickness for different assumptions of $\sigma_{\rho/\langle\rho\rangle}$ and $\langle A_V \rangle_{L_{\max}}$ as shown in Fig. 9.

It is possible that the turbulence varies from galaxy to galaxy. In a generalised model it prove useful to describe the turbulence by the mean value of the standard deviation $\sigma_{\rho/\langle\rho\rangle}$ and the optical thickness $\langle\tau\rangle_{L_{\max}}$ at one maximum scale. In this case the attenuation would be only a function of the slice thickness Δ/L_{\max} . A small attenuation is connected with a thin dust layer, a large attenuation with a thick dust layer. As shown in the paper the curvature will change with slice thickness through the turbulent medium. Therefore, the attenuation curve of a galaxy showing a relatively small attenuation should be characterised by a smaller R_V^A -value. Equally the attenuation curves of galaxies with high attenuation should be relatively flat with high R_V^A .

If we consider spiral galaxies the apparent thickness of the dust screen will vary with viewing angle. Therefore, the attenuation curve of a galaxy seen edge on should be flatter than the attenuation curve of a galaxy seen face on. The effect should be stronger for an ISM which is both more dense and more turbulent. It seems to be reasonable to assume that the largest turbulent scale L_{\max} is connected with the scale height of the galaxy so that the thickness of the dust screen of a galaxy seen face on should be around one maximum

scale. In this case the thickness should vary approximately as $\Delta \approx L_{\max} / \cos i$ where i is the viewing angle of the galaxy.

In general the situation for star-bursts and normal galaxies might be different as the star light in star-bursts is stronger related to HII-regions. In case of normal galaxies it might be important to consider a more realistic distribution of stars and dust. In spiral galaxies the old stars do, in general, have a greater scale height while young stars are more concentrated towards the galactic disc. In case of a young stellar population a foreground screen model might still be a reasonable approximation. For an old stellar population on the other hand it depends on the actual distribution of the dust and it is possible that a model where the stars are homogeneously mixed inside the turbulent medium is more appropriate. An additional complication might be the attenuation of the star light from the bulge. The importance of all these effects will depend on the contribution of the different stellar populations to the intrinsic star light of the galaxy.

5.2.1. The 'Calzetti-extinction-law'

Let us consider the empirical curve derived for star-burst galaxies. We assume a turbulent density structure with $n = -10/3$ and a scaling relation extending over several magnitudes. As shown in Sect. 3 the relative attenuation \mathcal{E}_λ suggests $R_V \sim 4.3$. We ignore the discrepancy at short wavelengths as this is possibly due to the destruction of PAH-molecules which are believed to be the carriers of the 2200 Å bump in star bursts. We already discussed this issue in Paper I and in more detail in Dopita et al. (2005).

The observations of star-bursts show that the effective optical depth varies quite strongly from galaxy to galaxy. Following Calzetti (2001) the attenuation A_V lies in the range from 0.20 to 2.23 with a mean of 0.63¹.

Using the approximation of a thick slice and assuming that the dust screen has a thickness of at least one maximum scale L_{\max} then the lower limit of the standard deviation $\sigma_{\rho/\langle\rho\rangle}$ is in the range 2 to 6. If the turbulence of these galaxies is similar the standard deviation of the local density should be at least ~ 6 .

From the variation of R_V^A with slice thickness (Fig. 9) we must conclude that the turbulence must be characterised by a standard deviation $\sigma_{\rho/\langle\rho\rangle} > 1$ since none of the cases considered with $\sigma_{\rho/\langle\rho\rangle} = 1$ can reproduce the observational results of $R_V^A = 4.3$ and a mean

¹We have taken the attenuation A_B (Table 4, Calzetti (2001)) and used an R_V^A -value of 4.05 as stated in the text to obtain A_V .

attenuation of $A_V = 0.63$.

For $\sigma_{\rho/\langle\rho\rangle} = 2.5$ the slice thickness has to be very thin if the mean value of $A_V = 0.63$ is to be consistent with the observed value, $R_V^A \sim 4.3$. More likely we require a standard deviation of at least $\sigma_{\rho/\langle\rho\rangle} \sim 5.0$ to explain the observed R_V^A . With these parameters the thickness of the dust screen is only slightly larger than one maximum scale and $\langle A_V \rangle_{L_{\max}} \sim 0.6$. The variation of the attenuation A_V can be explained by different values of the slice thickness Δ/L_{\max} ranging from ~ 0.4 to ~ 6 and may partly be caused by the different inclination angles of the galaxies. As seen in Fig. 9 the variation of the attenuation A_V should be connected with different attenuation curves with R_V^A -values in the range from ~ 4 to ~ 4.5 .

Wider distributions of the local density require lower optical depths and thicker dust layers. In case of $\sigma_{\rho/\langle\rho\rangle} = 7.5$ the attenuation curve of star-bursts can be reproduced if $\langle A_V \rangle_{L_{\max}} \approx 0.3$. The slice thickness varies from ~ 0.9 to ~ 11 changing R_V^A from ~ 4.1 to ~ 4.5 . The mean thickness is ~ 3 .

As can be seen in Fig. 9 the ‘Calzetti-curve’ can also be reproduced in a turbulent medium with $\sigma_{\rho/\langle\rho\rangle} = 10$. In this case $\langle A_V \rangle_{L_{\max}} \approx 0.15$. The dust screen would have a thickness ranging from ~ 2 to ~ 22 with a mean of ~ 6 and R_V^A would vary from 4 to 4.4. If we identify the lower limit of the attenuation with galaxies seen face on and require that its dust screen is not larger than one maximum scale we can conclude that the standard deviation of the local density has to be smaller than $\sigma_{\rho/\langle\rho\rangle} = 10$.

Based on this analysis the ‘Calzetti-curve’ implies a standard deviation of the local density of order ~ 7.5 , only slightly larger than the minimum value derived by using the thick slice approximation. However, one has to bear in mind that due to the strong UV-radiation the dust properties in star-bursts may be different to the ones of the ISM of our galaxy. Nonetheless, the interpretation is probably still correct because the extinction curve up to 4400 Å should not be strongly effected by such variations, if mainly due to the presence or absence of PAH molecules.

A thin slice with a thickness much less than the largest scale would imply that the turbulent medium is mixed with the stars. In this case the model of a distant foreground screen is somewhat questionable and another approach may be more appropriate. If the scattered light makes only a very small contribution it is still a reasonable assumption to consider the dust layers in front of each layer of stars as a distant foreground screen. The effective attenuation curve of such a medium is obtained by comparing the whole transmitted light with the light emitted inside the screen.

By fitting the ‘Calzetti-extinction-curve’ with the turbulent foreground screen model we found that the minimum Mach number is in the range 1.3 to 22 if relation 1 applies. This

is consistent with the Mach numbers found for the WNM and CNM in our own galaxy (see Sect. 2).

The fact that the standard deviation $\sigma_{\rho/\langle\rho\rangle}$ of the turbulent screen has to be significantly larger than unity to explain the ‘Calzetti-extinciton-law’ would imply that the Mach number, assuming the relation 1 applies, has to be larger than 2, i.e. larger than the Mach number of the WNM of our galaxy. On the other hand, the range for $\sigma_{\rho/\langle\rho\rangle}$ which is consistent with the attenuation observed for star burst galaxies would imply Mach numbers in the range 10 to 15. This suggest that the attenuation of star burst galaxies is caused by the structure related to the turbulent CNM.

It is likely, that at the epoch of galaxy formation, galaxies were more violent systems characterised by a wider distribution of the local density (larger $\sigma_{\rho/\langle\rho\rangle}$) and by a higher mean optical thickness $\langle\tau\rangle_{L_{\max}}$. These systems will therefore probably have attenuation curves which are flatter than the curve derived for local star-bursts.

5.3. Limitations

An obvious limitation of these models is the fact that scattered light is not taken into account. It may also be more realistic to consider other geometries where the stars are connected with the turbulent dust screen or mixed with the turbulent ISM. By including scattering we expect that the attenuation curve will be slightly lower where the scattered light makes a large contribution to the total extinction which is the case in the UV. But as we outlined in paper I the light scattered out of the observed direction cannot be totally compensated by scattered light from other stars. To understand how far our simple model can be applied to explain the attenuation for different geometries it will still be important to study the effects of scattering quantitatively.

It may also be important to consider the variation of dust properties with local density, radiation field and stellar population and to understand how these variations affect the mean extinction curve. However, since these effects are not sufficiently understood it may still be better to assume a mean extinction curve of our own galaxy and to use the attenuation curves presented in this paper.

6. Summary

We have analysed in detail the attenuation curve caused by a distant isothermal turbulent dust screen. We used a simplified model of the turbulent medium based on its statistical

properties where the PDF of the local density is log-normal and the power spectrum a simple power law. The turbulence is assumed to extend from a maximum scale L_{\max} down to a minimum scale L_{\min} . The optical depth is taken to be proportional to the column density and the PDF of the column density to be log-normal. The attenuation curve is derived using the mean extinction curve of our galaxy as provided by Weingartner & Draine (2001).

The main results are:

1. The attenuation curves in isothermal turbulent dusty media are determined by the absolute-to-relative attenuation ratio R_V^A and the absolute attenuation A_V . The R_V^A -value determines the curvature while A_V the scaling. A higher R_V^A -value relates to a flatter attenuation curve.
2. The absolute-to-relative attenuation ratio R_V^A increases with slice thickness.
3. For slices much thicker than the maximum scale L_{\max} the R_V^A -value converges towards a maximum value. The attenuation curve becomes independent on slice thickness.

The R_V^A -value depends on the structure, the PDF of the local density and the mean value of the optical thickness of the dust screen. The dependence of single parameters characterising the turbulent slice is as follows:

1. The R_V^A -value increases with optical thickness.
2. More turbulent media, characterised by a broader PDF or a higher standard deviation $\sigma_{\rho}/\langle \rho \rangle$ of the local density, are characterised by higher R_V^A -values (assuming that the structure is the same). The attenuation is smaller in such media.
3. Turbulence characterised by a broader correlation function (steeper power spectrum) leads to a higher R_V^A -value as a result of a broader PDF of the optical depths.
4. The curvature of the attenuation curve depends on the ratio $\zeta = L_{\max}/L_{\min}$. For higher values of ζ the PDF of the column density becomes narrower and therefore the effect due to turbulence smaller: The R_V^A -value becomes smaller and the attenuation A_V larger. The effect is particularly important in turbulent media with $n \leq -3$. In the limit of $\log_{10} \zeta \gg 1$ the effect due to turbulence would disappear. For Kolmogorov turbulence (or general $n < -3$) the R_V^A -value will reach a lower limit.

M. Dopita acknowledges the support of the ARC and the Australian National University through his Australian Federation Fellowship. Both authors acknowledge financial support for this research through ARC Discovery project DP0208445.

REFERENCES

Calzetti, D., Kinney, A. L., & Storchi-Bergmann, T., 1994, ApJ 429, 582

Calzetti, D. 2001, PASP, 113, 1449

Dopita, M. et al. 2005 ApJ, in press

Fischera, J., Dopita, M., Sutherland, R., 2003, ApJL 599, L21

Fischera, J., Dopita, M., 2004 ApJ 611, 919

Iroshnikov, P., 1964, Astron. Zh. 40, 742

Kraichnan, R., 1965, Phys. Fluids 8, 1385

Nordlund, Å., & Padoan, P. 1999, in Insterstellar Turbulence, ed. J. Franco & A. Carriñana, (Cambridge: Cambridge Univ. Press), 218

Ostriker, E.C., Stone, J.M., & Gammie, C.F. 2001, ApJ546, 980

Padoan, J., Jones, B.T., & Nordlund, Å.P. 1997, ApJ474, 730

Passot, T., & V'azquez-Semadeni, E., 1998. Phys. Rev. E 58, 4501

Vázquez-Semadeni, E., 1994, ApJ 423, 681

Weingartner, J. C. & Draine, B. T. 2001, ApJ, 548, 296

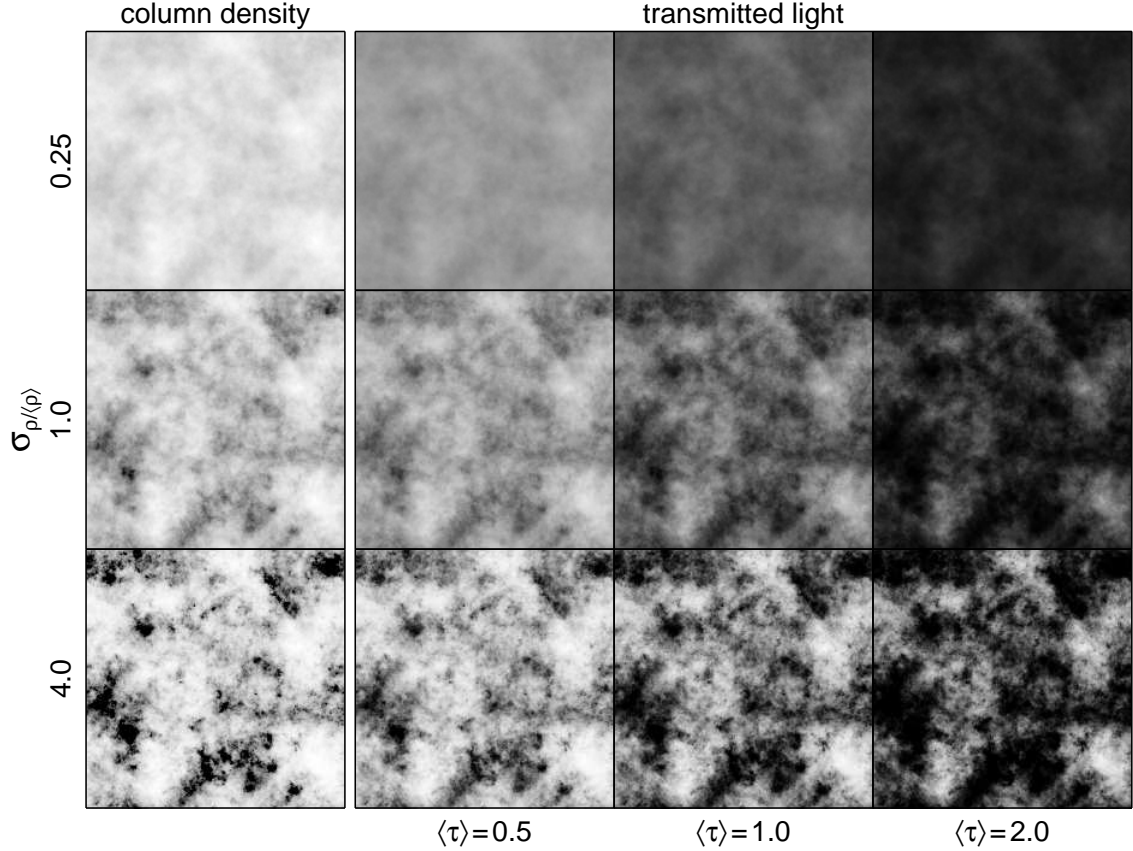


Fig. 1.— Visualisation of the attenuation caused by a turbulent distant screen. The turbulent density structure has been derived using a volume of $216^2 \times 108$ pixels. The thickness of the screen is taken to be one maximum scale L_{\max} and the width of the screen area is chosen to be two maximum scales. The power spectrum of the normal distributed density values is taken to be Kolmogorov. The first column shows the column density per pixel for three different values of the standard deviation $\sigma_{\rho/\langle\rho\rangle}$ of the local density. Bright regions are locations of low column densities, dark regions of high column densities. The values are linearly scaled from the minimum to the maximum value of the column densities obtained for a density structure with $\sigma_{\rho/\langle\rho\rangle} = 1$. The transmitted light of the screens is shown in column 2 to 4 for three different values of the mean optical depth $\langle\tau\rangle$. The grey tone represents the amount of transmitted light. Bright regions correspond to small extinction, dark regions to high extinction.

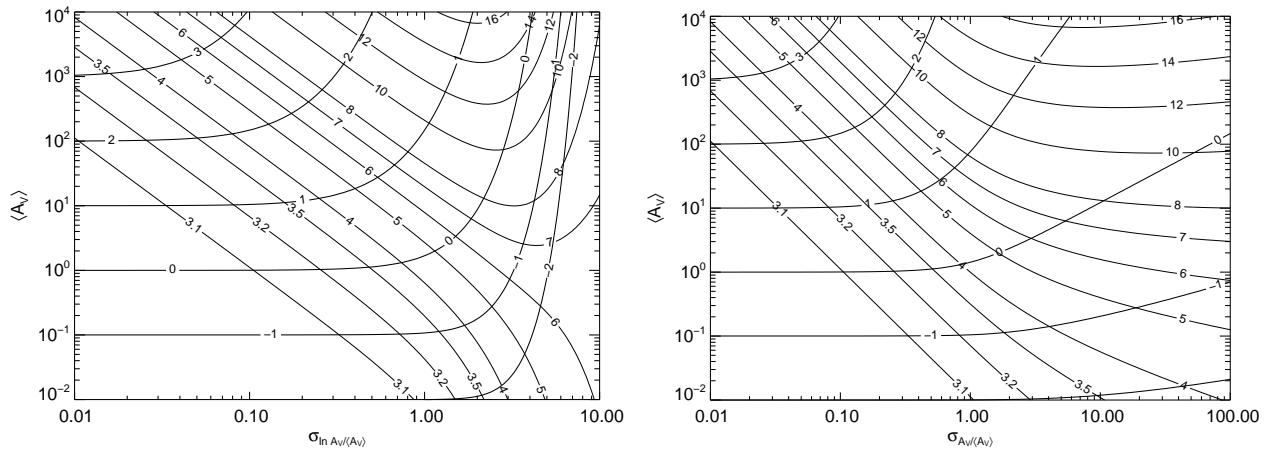


Fig. 2.— Attenuation A_V (thick solid lines) as a function of the averaged attenuation $\langle A_V \rangle$ and the standard deviation $\sigma_{\ln A_V / \langle A_V \rangle} = \sigma_{\ln \tau_V / \langle \tau_V \rangle}$ (left hand figure) and as a function of the averaged attenuation $\langle A_V \rangle$ and the standard deviation $\sigma_{A_V / \langle A_V \rangle} = \sigma_{\tau_V / \langle \tau_V \rangle}$ (right hand figure). The label values correspond to $\log A_V$. Also shown are lines of constant values of the absolute-to-relative attenuation ratio $R_V^A = A_V / E(B - V) = \tau_V / (\tau_B - \tau_V)$.

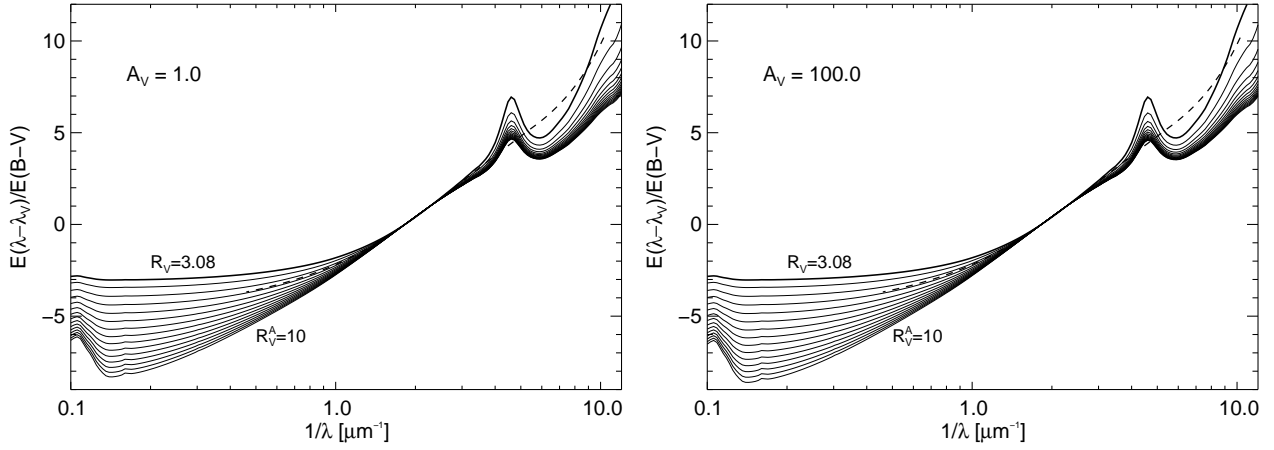


Fig. 3.— Relative attenuation curves $E(\lambda - \lambda_V)/E(B - V)$ for various values R_V^A varied from 3.5 up to 10 with $\Delta R_V^A = 0.5$. The attenuation A_V is constant chosen to be 1.0 and 100.0, respectively. As can be seen in Fig. 2 the conditions of the foreground screen (the mean attenuation $\langle A_V \rangle$ and the contrast $\sigma_{\ln \tau}$ of the optical depths) which lead to the same R_V^A in the left and in the right hand figure are different. The thick solid line is the initial extinction curve provided by Weingartner & Draine (2001) where $R_V = 3.08$. For comparison the attenuation curve derived for star burst galaxies (broken line) is shown (Calzetti (2001)).

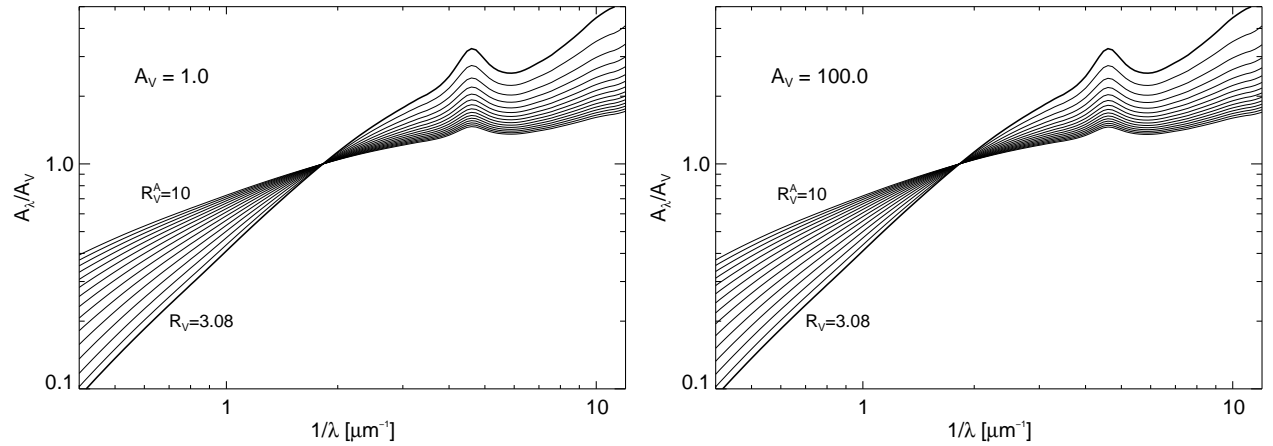


Fig. 4.— Attenuation curves A_λ/A_V caused by a distant turbulent dust screen varying R_V^A from 3.5 to 10. The difference in R_V^A between neighboured curves is taken to be 0.5. Also shown is the initial mean extinction curve with $R_V = 3.08$ (thick solid line).

Table 1. Relative attenuation $E(\lambda - V)/E(B - V)$ for various values of R_V^A

$\lambda[\mu\text{m}]$	remark	$R_V = 3.08$	$R_V^A = 3.5$	$R_V^A = 4.0$	$R_V^A = 4.5$	$R_V^A = 5.0$	$R_V^A = 5.5$	$R_V^A = 6.0$	$R_V^A = 7.0$	$R_V^A = 8.0$	$R_V^A = 9.0$	$R_V^A = 10$
$A_V = 1$												
0.0912	Ly ∞	12.066	9.716	8.675	8.113	7.750	7.490	7.294	7.014	6.822	6.680	6.570
0.1053		9.694	8.105	7.349	6.932	6.659	6.463	6.314	6.100	5.953	5.844	5.759
0.1216	Ly α	7.328	6.385	5.898	5.621	5.437	5.303	5.202	5.055	4.953	4.878	4.820
0.1550	C IV	5.018	4.573	4.3109	4.169	4.068	3.994	3.937	3.854	3.796	3.754	3.720
0.1906	C III	5.214	4.732	4.460	4.300	4.192	4.113	4.053	3.965	3.903	3.858	3.822
0.2175	2175	6.937	6.088	5.643	5.388	5.219	5.096	5.002	4.866	4.772	4.702	4.648
0.2480		4.573	4.206	3.992	3.865	3.779	3.715	3.667	3.596	3.546	3.509	3.480
0.3000		2.967	2.827	2.738	2.684	2.646	2.618	2.596	2.564	2.541	2.515	2.511
0.3650	U	1.924	1.880	1.849	1.830	1.817	1.807	1.799	1.787	1.779	1.773	1.768
0.440	B	1.000	1.000	1.000	1.000	1.000	1.000	1.000	1.000	1.000	1.000	1.000
0.548	V	0.000	0.000	0.000	0.000	0.000	0.000	0.000	0.000	0.000	0.000	0.000
0.720	R	-0.991	-1.048	-1.098	-1.134	-1.162	-1.184	-1.201	-1.228	-1.248	-1.263	-1.274
1.030	I	-1.871	-2.035	-2.197	-2.323	-2.424	-2.507	-2.575	-2.682	-2.761	-2.823	-2.872
1.239	J	-2.171	-2.386	-2.607	-2.786	-2.934	-3.056	-3.159	-3.322	-3.445	-3.542	-3.619
1.649	H	-2.498	-2.777	-3.078	-3.336	-3.557	-3.746	-3.909	-4.173	-4.376	-4.537	-4.668
2.192	K	-2.716	-3.044	-3.413	-3.741	-4.034	-4.293	-4.521	-4.900	-5.199	-5.440	-5.638
3.592	L	-2.932	-3.312	-3.759	-4.179	-4.575	-4.944	-5.283	-5.877	-6.371	-6.783	-7.128
4.777	M	-2.992	-3.388	-3.859	-4.310	-4.745	-5.158	-5.547	-6.250	-6.852	-7.364	-7.800
$A_V = 10$												
0.0912	Ly ∞	12.066	9.686	8.602	8.015	7.636	7.369	7.169	6.888	6.698	6.561	6.456
0.1053		9.694	8.085	7.298	6.861	6.576	6.373	6.221	6.005	5.859	5.753	5.673
0.1216	Ly α	7.328	6.374	5.866	5.575	5.383	5.244	5.140	4.991	4.890	4.816	4.760
0.1550	C IV	5.018	4.568	4.303	4.146	4.040	3.962	3.903	3.819	3.761	3.719	3.687
0.1906	C III	5.214	4.726	4.443	4.275	4.162	4.080	4.017	3.927	3.866	3.821	3.787
0.2175	2175	6.937	6.078	5.614	5.347	5.169	5.041	4.945	4.859	4.713	4.645	4.593
0.2480		4.573	4.202	3.979	3.846	3.755	3.689	3.638	3.566	3.516	3.480	3.452
0.3000		2.967	2.826	2.733	2.676	2.636	2.606	2.584	2.551	2.528	2.511	2.499
0.3650	U	1.924	1.879	1.848	1.827	1.813	1.803	1.794	1.782	1.774	1.768	1.763
0.440	B	1.000	1.000	1.000	1.000	1.000	1.000	1.000	1.000	1.000	1.000	1.000
0.548	V	0.000	0.000	0.000	0.000	0.000	0.000	0.000	0.000	0.000	0.000	0.000
0.720	R	-0.991	-1.049	-1.100	-1.138	-1.168	-1.191	-1.209	-1.238	-1.258	-1.273	-1.285
1.030	I	-1.871	-2.038	-2.201	-2.333	-2.441	-2.529	-2.602	-2.716	-2.799	-2.863	-2.913
1.239	J	-2.171	-2.390	-2.612	-2.799	-2.956	-3.087	-3.197	-3.372	-3.502	-3.602	-3.681
1.649	H	-2.498	-2.781	-3.084	-3.350	-3.583	-3.786	-3.961	-4.244	-4.461	-4.631	-4.767
2.192	K	-2.716	-3.049	-3.417	-3.755	-4.061	-4.336	-4.580	-4.990	-5.312	-5.569	-5.777
3.592	L	-2.932	-3.318	-3.761	-4.188	-4.595	-4.979	-5.339	-5.978	-6.515	-6.959	-7.327
4.777	M	-2.992	-3.394	-3.860	-4.316	-4.758	-5.185	-5.593	-6.342	-6.993	-7.544	-8.006

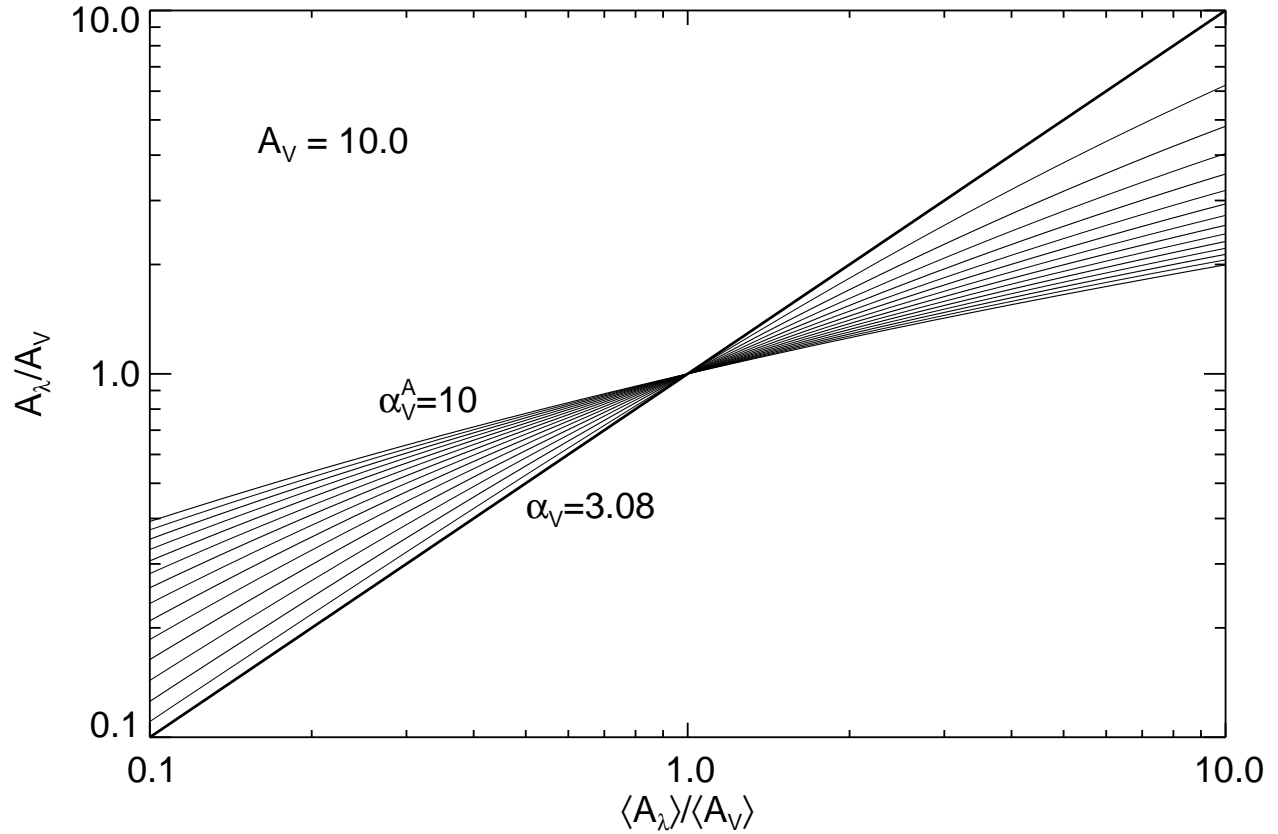


Fig. 5.— Attenuation A_λ/A_V of a turbulent screen as function of the extinction $\langle A_\lambda \rangle / \langle A_V \rangle = k_\lambda/k_V$. The absolute attenuation has been chosen to be $A_V = 10$. The result, however, depends primarily on the ratio on the absolute to relative attenuation $\alpha_V^A = A_V/E(\tilde{\lambda} - V)$ where the extinction coefficient at wavelength $\tilde{\lambda}$ has to fulfil $\alpha_V = k_V/(k_{\tilde{\lambda}} - k_V) = 3.08$. α_V^A is varied from 3.5 to 10 in steps of 0.5.

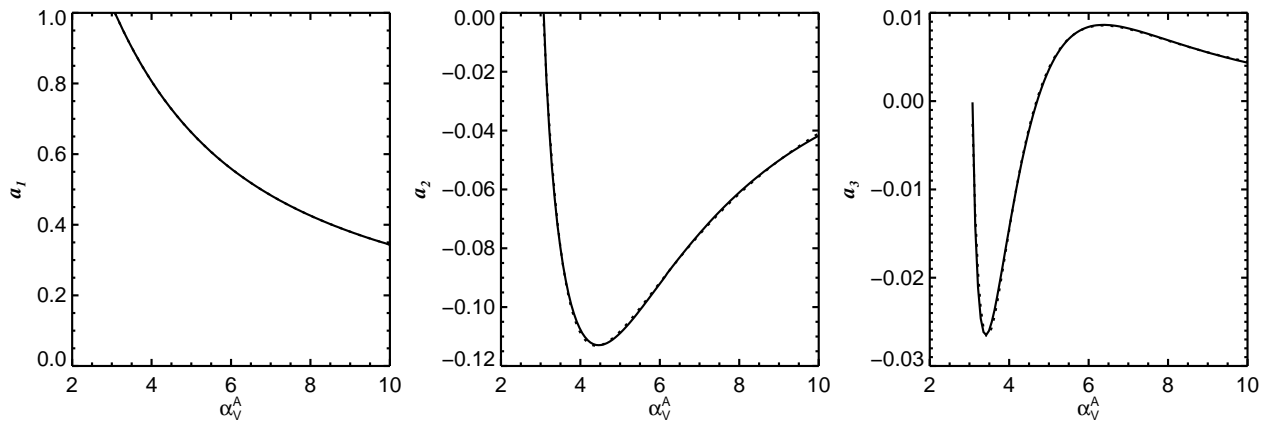


Fig. 6.— Coefficients a_1 , a_2 , and a_3 of the approximation of $\log A_\lambda/A_V$ as function of the absolute-to-relative attenuation ratio α_V^A (solid lines) using a polynomial function of third order (Eq. 8). The dotted line, which can be barely distinguished from the solid line in these panels, is a fit using the polynomial function given in Eq. 9. The attenuation chosen for this figure is $A_V = 1$. However, the functional form obtained for $A_V = 10$ is very similar.

Table 2. Coefficients of the Polynomial Approximation of the Attenuation Curve

	b_0	b_1	b_2	b_3	b_4
$A_V = 1.0$					
a_1	0.00495676	3.42939	-3.62163	1.64220	—
a_2	0.0393932	-0.708645	-0.668874	5.11725	-2.19900
a_3	0.0174931	-0.484444	5.17489	-19.2137	21.5465
$A_V = 10.0$					
a_1	0.00117052	3.49788	-3.87317	1.90329	—
a_2	0.0717661	-1.40474	2.76259	-1.30223	1.96333
a_3	-0.0163800	0.186388	1.30772	-10.5378	14.8253

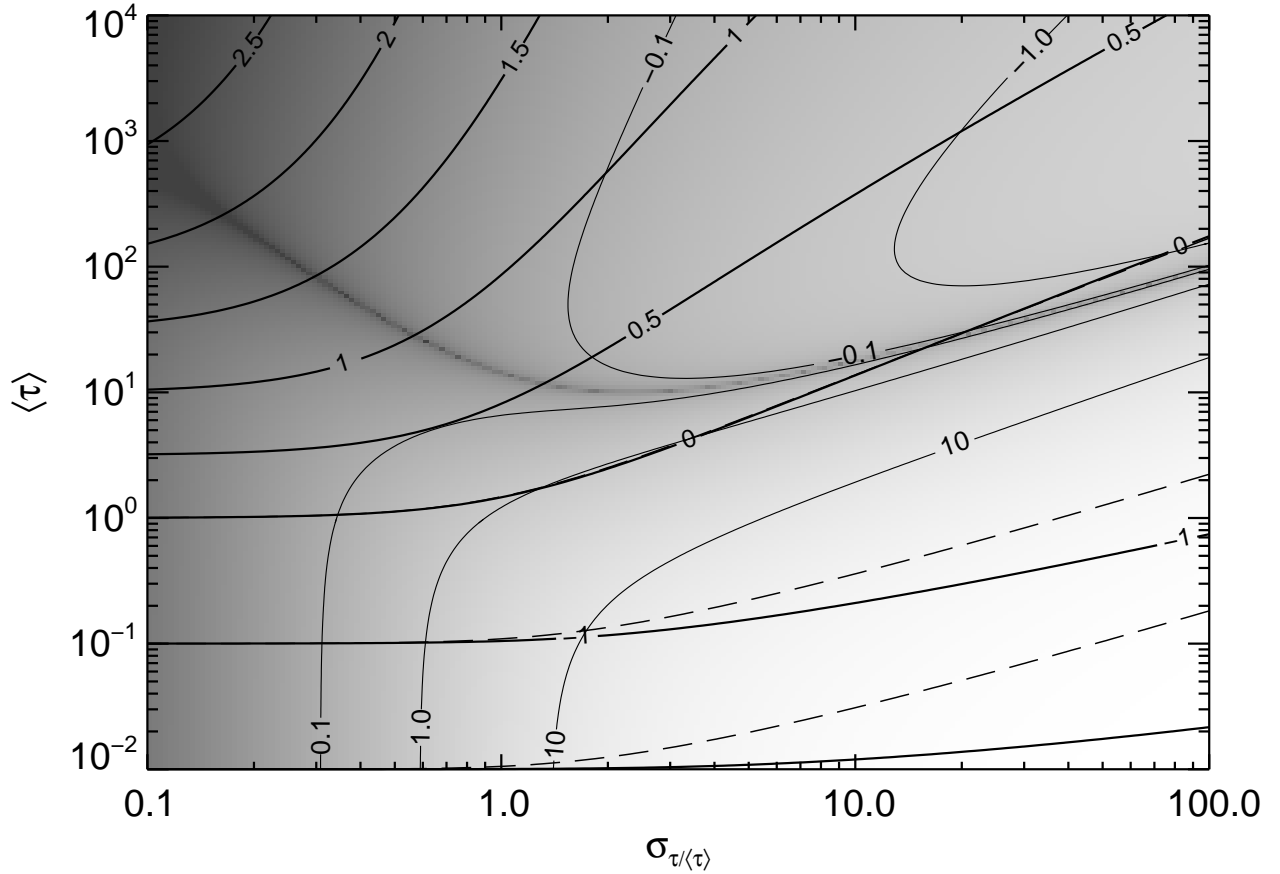


Fig. 7.— Accuracy of the approximation Eq. 13 of the effective optical depth τ_{eff} shown in grey scale where the accuracy increases towards darker colour. The accuracy of 0.1, 1.0, and 10.0% is shown as thin contour lines. Along the dark stripe the approximation gives the correct value. Above this curve the correct values are generally smaller while they are larger otherwise. The thick and dashed lines refer to constant effective optical depths derived by calculating the integral 4 and by using the approximation 13.

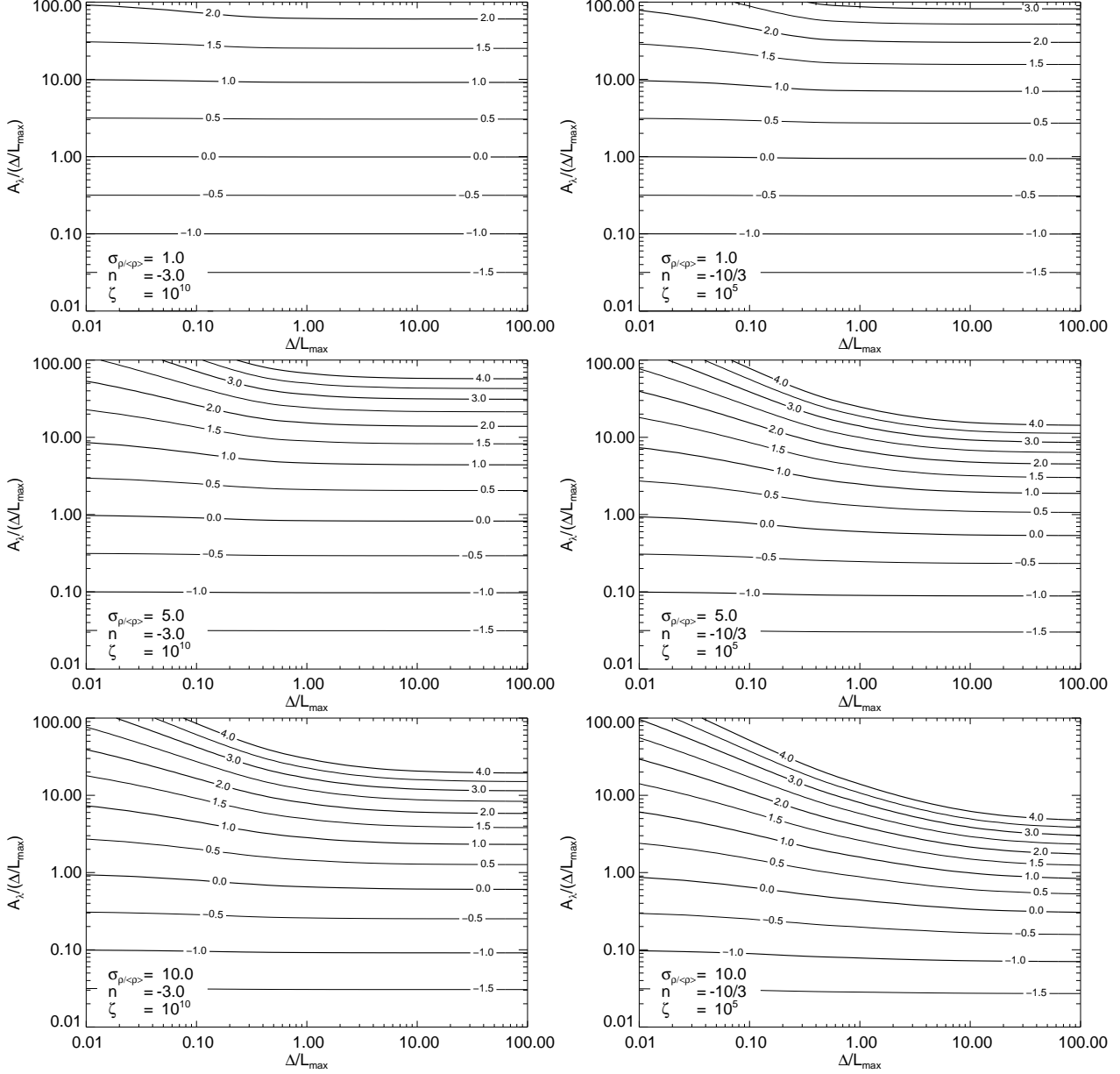


Fig. 8.— Attenuation $A_\lambda / (\Delta L_{\max})$ as function of slice thickness for a foreground turbulent screen with $\sigma_{\rho/\langle\rho\rangle} = 1.0, 5.0$, and 10.0 . The different curves correspond to different cases of the mean attenuation $\langle A_\lambda \rangle_{L_{\max}}$ varied from $10^{-1.5}$ to 10^4 . The power index of the power spectrum is taken to be $n = -3$ and $n = -10/3$ with $\zeta = 10^{10}$ and $\zeta = 10^5$, respectively.

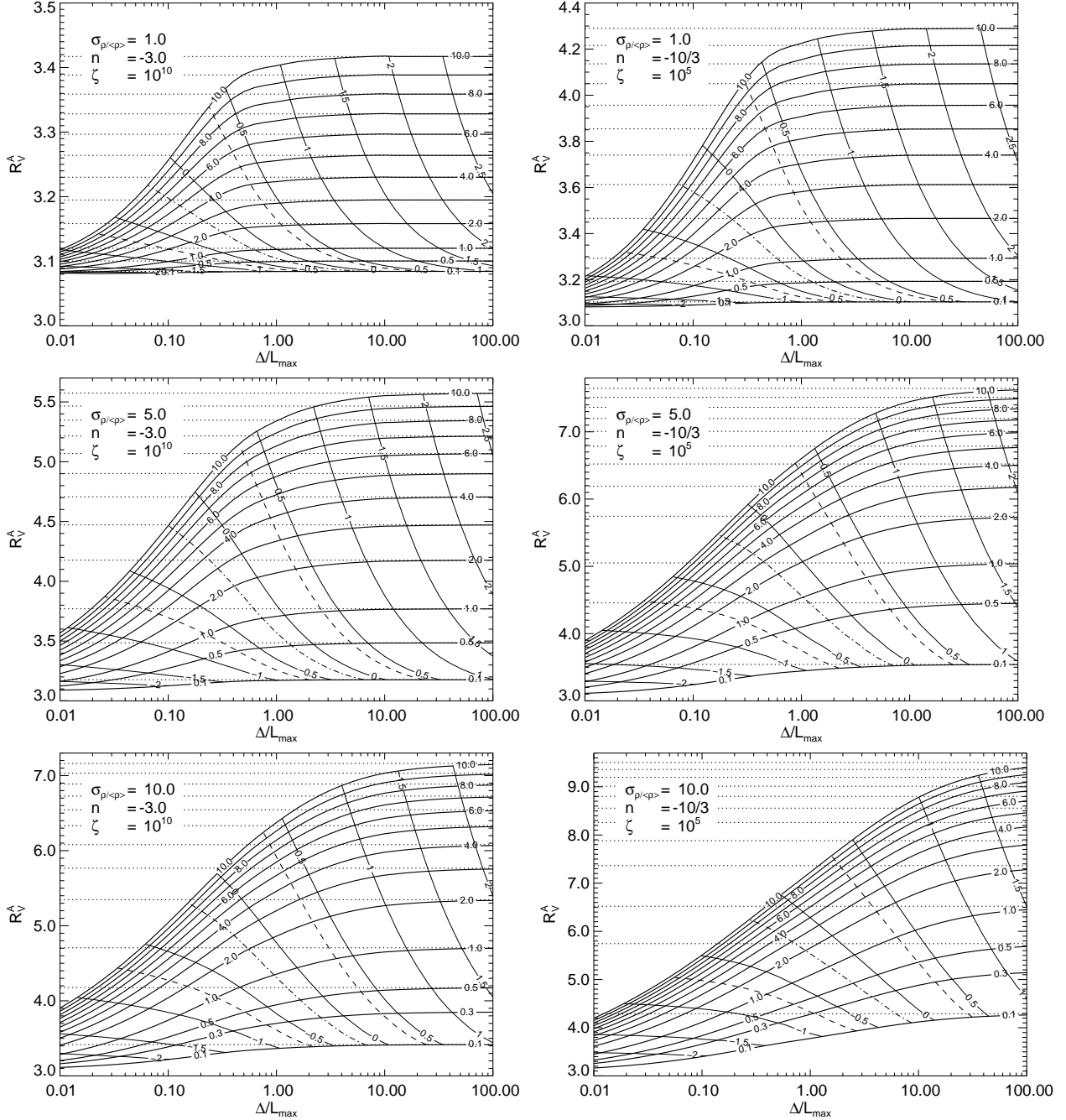


Fig. 9.— Variation of the absolute-to-relative attenuation ratio R_V^A with slice thickness Δ/L_{\max} (thick solid lines). The curves are labelled with the assumed attenuation $\langle A_V \rangle_{L_{\max}}$ at one maximum scale L_{\max} ranging from 0.1 up to 10.0. The attenuation A_V is shown as thin solid lines. Those curves are labelled with $\log A_V$. Also shown as dashed, dashed dotted, and dashed curves are a minimum, mean and maximum value of A_V as derived for star-burst galaxies Calzetti (2001). The dotted lines visualise the R_V^A -value in the limit of thick slices using equation 16. The power spectrum is again assumed to have $n = -3$ and $n = -10/3$ with $\zeta = 10^{10}$ and $\zeta = 10^5$, respectively. The standard deviation of the local density is varied from 1.0, 5.0 to 10.0.

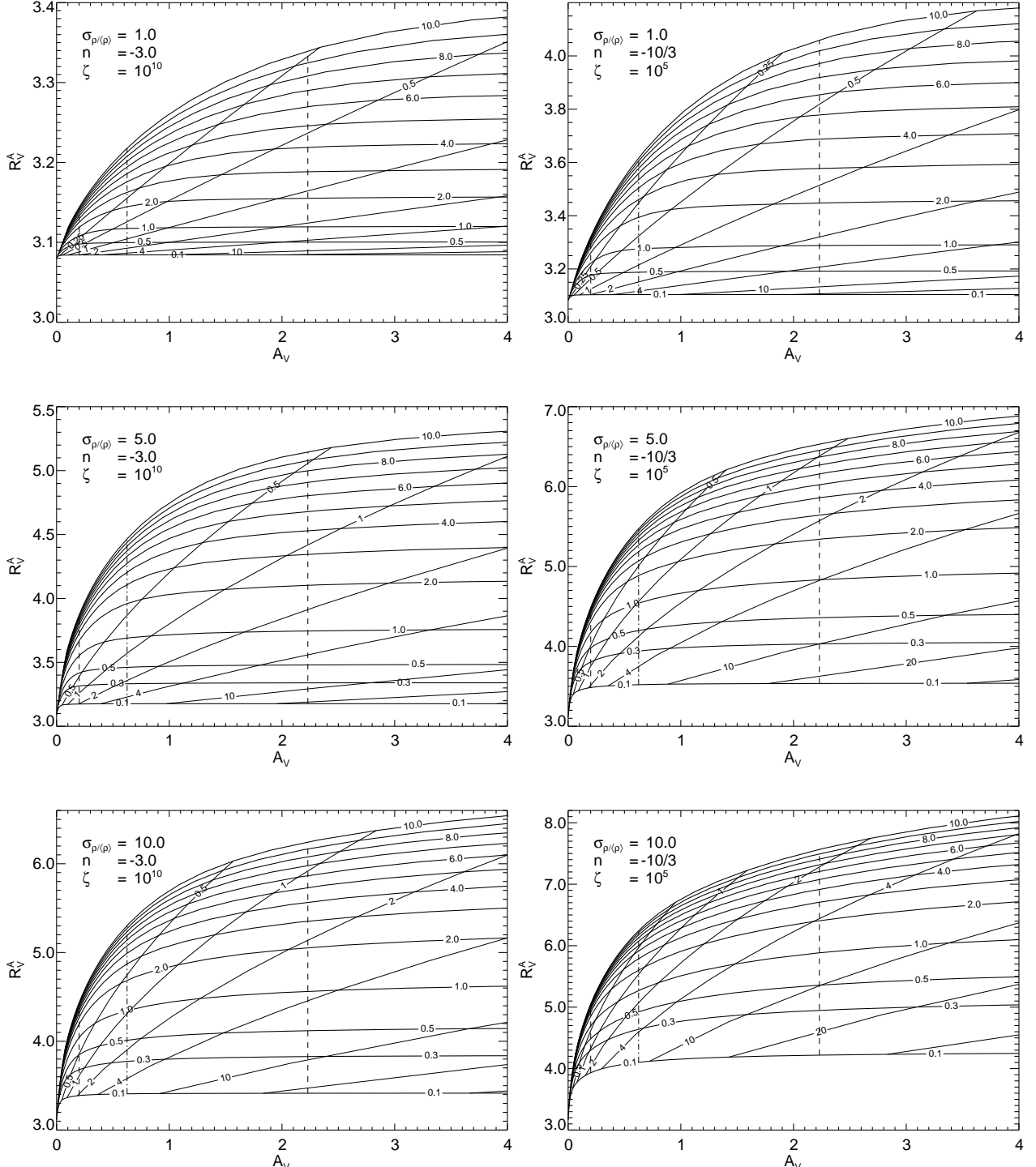


Fig. 10.— Absolute-to-relative attenuation ratio R_V^A as function of the measurable attenuation A_V for different assumptions of the distant turbulent screen. The curves shown as thick lines correspond to certain values of the mean attenuation $\langle A_V \rangle_{L_{\max}}$ at one maximum turbulent scale varied from 0.1 to 10. The thickness Δ/L_{\max} of the screen is shown as thin lines. The power is again assumed to be -3 or $-10/3$ with a scaling relation ranging over 10 and 5 magnitudes. The standard deviation of the local density is again chosen to be 1, 5, and 10. For comparison also the range of the attenuation measured for star burst galaxies is shown, given as broken lines. The dashed-dotted line is its mean value.

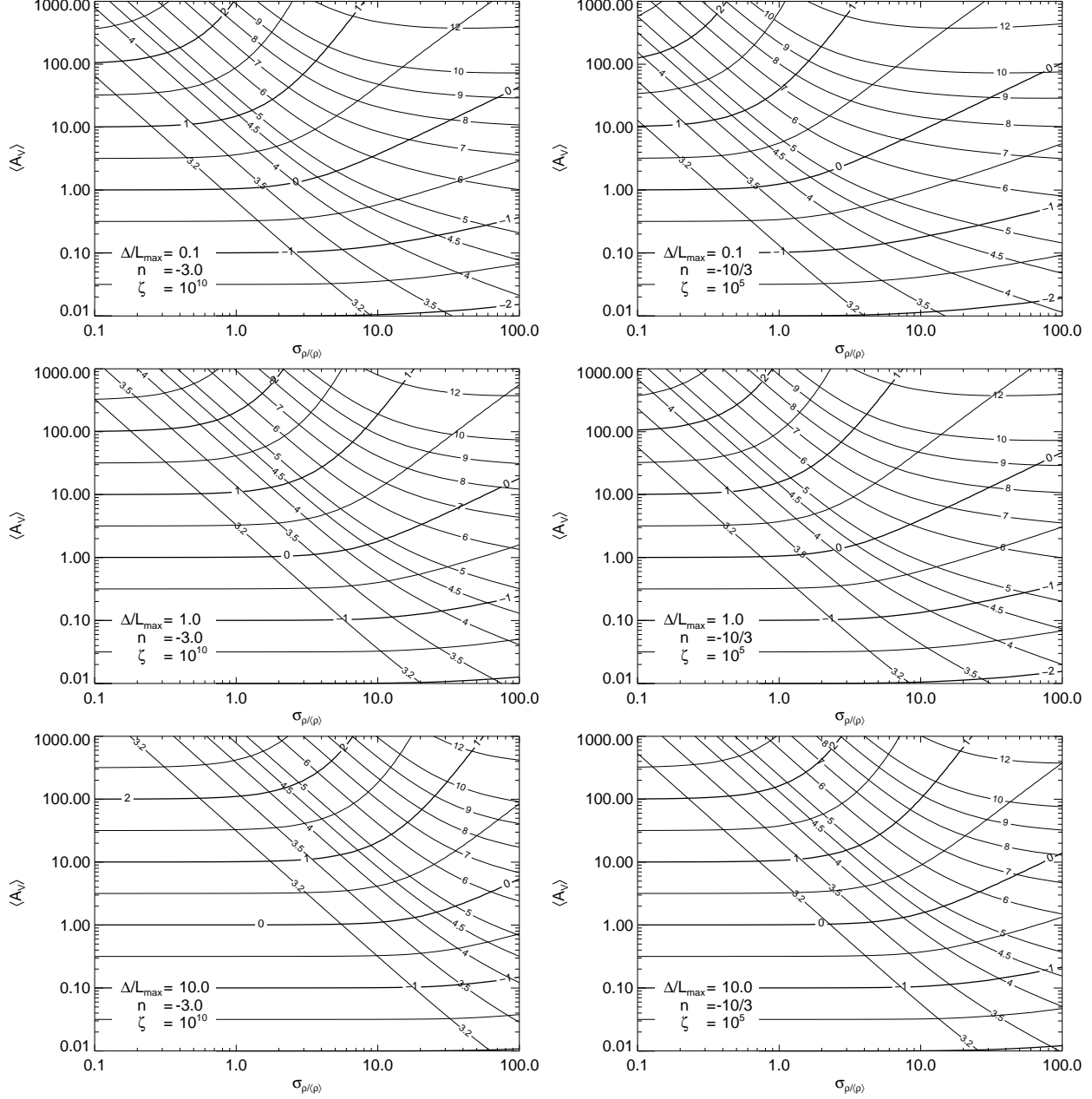


Fig. 11.— Attenuation A_V in V as function of the standard deviation $\sigma_{\rho/\langle \rho \rangle}$ of the local density and the mean attenuation $\langle A_V \rangle$ for three slices of different thickness where Δ/L_{\max} is chosen to be 0.1, 1.0, and 10.

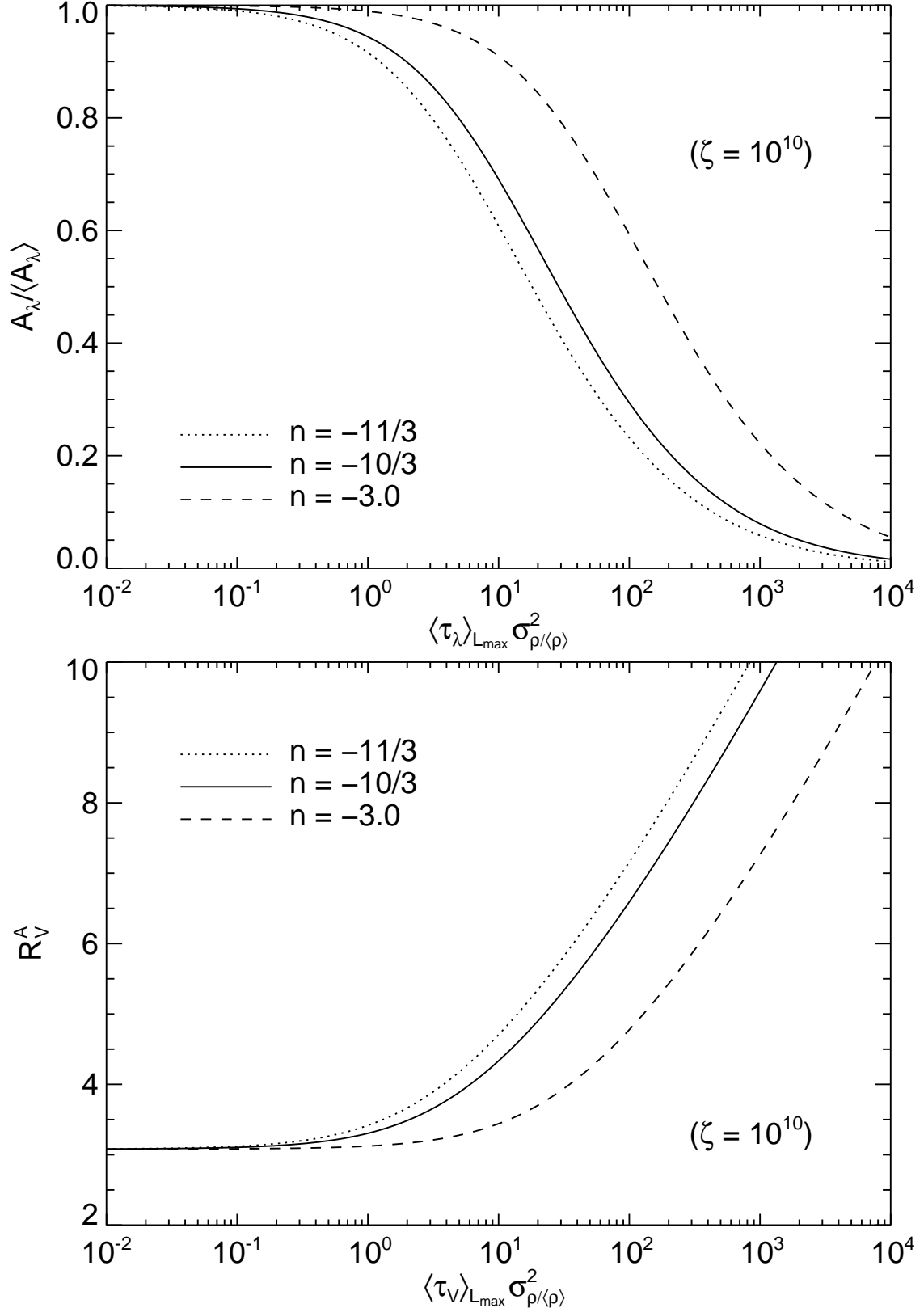


Fig. 12.— Ratio $A_\lambda / \langle A_\lambda \rangle$ as a function of $\langle \tau_\lambda \rangle_{L_{\max}} \sigma_{\rho/\langle \rho \rangle}^2$ and R_V^A as a function of $\langle \tau_V \rangle_{L_{\max}} \sigma_{\rho/\langle \rho \rangle}^2$ in the limit of slices with $\sigma_{\tau/\langle \tau \rangle}^2 \ll 1$. The turbulence is assumed to extend over $\zeta = 10^{10}$ scales.

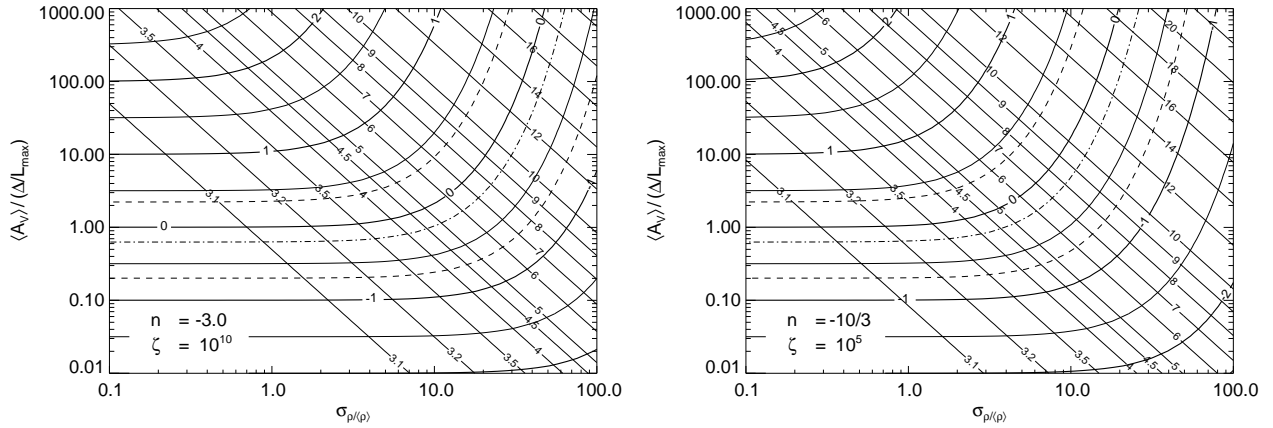


Fig. 13.— Attenuation $A_V / (\Delta L_{\max})$ (thick lines) as function of $\sigma_{\rho/\langle \rho \rangle}$ and $\langle A_V \rangle / (\Delta L_{\max})$ in the limit of thick slices with $\Delta L_{\max} \gg 1$. The absolute-to-relative attenuation R_V^A is shown as thin solid lines. Also shown are minimum, mean, and maximum values of the attenuation A_V derived for star-burst galaxies (dashed, dashed dotted, and dashed line) (Calzetti 2001).

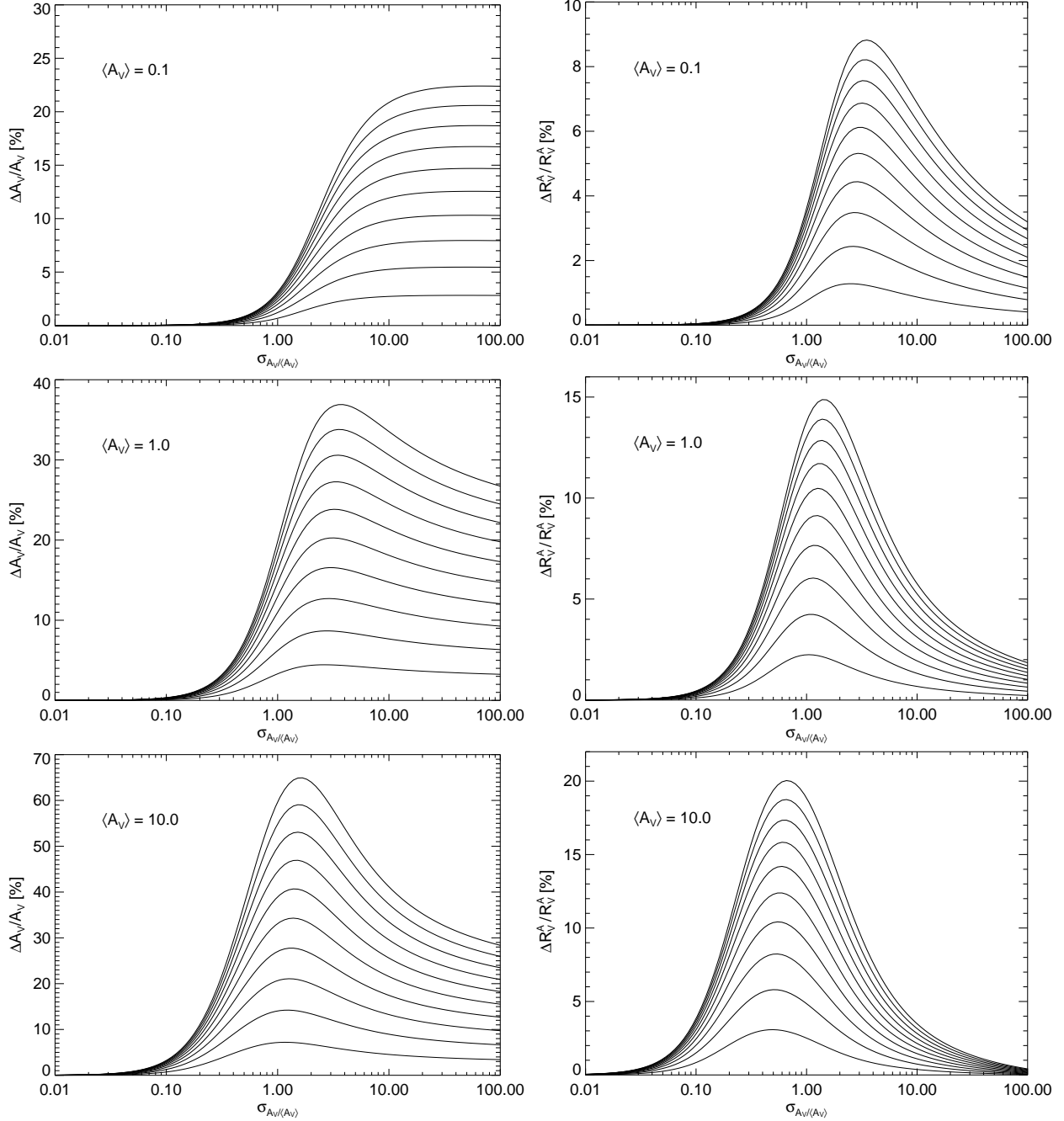


Fig. 14.— Accuracy of the derived observable quantities A_V and R_V^A for different assumptions of the uncertainty of the standard deviation $\sigma_{A_V}/\langle A_V \rangle$ and the mean value $\langle A_V \rangle$. The standard deviation of the column density is assumed to be up to 100% too large in comparison with the correct value. The difference in the assumed error for two neighbouring curves is 10%. The uncertainty of A_V and R_V^A increases with increasing error in the standard deviation $\sigma_{A_V}/\langle A_V \rangle$.

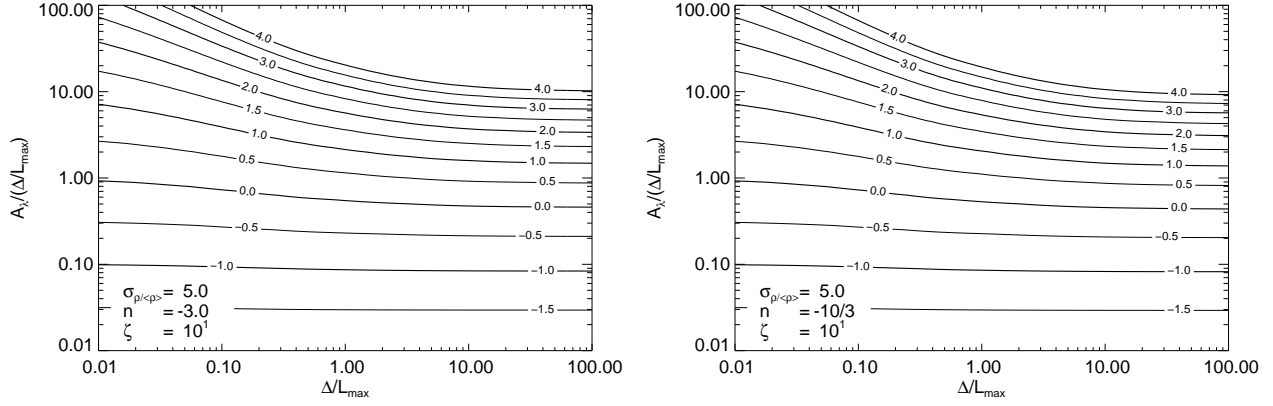


Fig. 15.— Same as plot for $\sigma_{\rho/\langle\rho\rangle}$ in Fig. 8 but assuming a turbulent medium with only $\zeta = 10$.

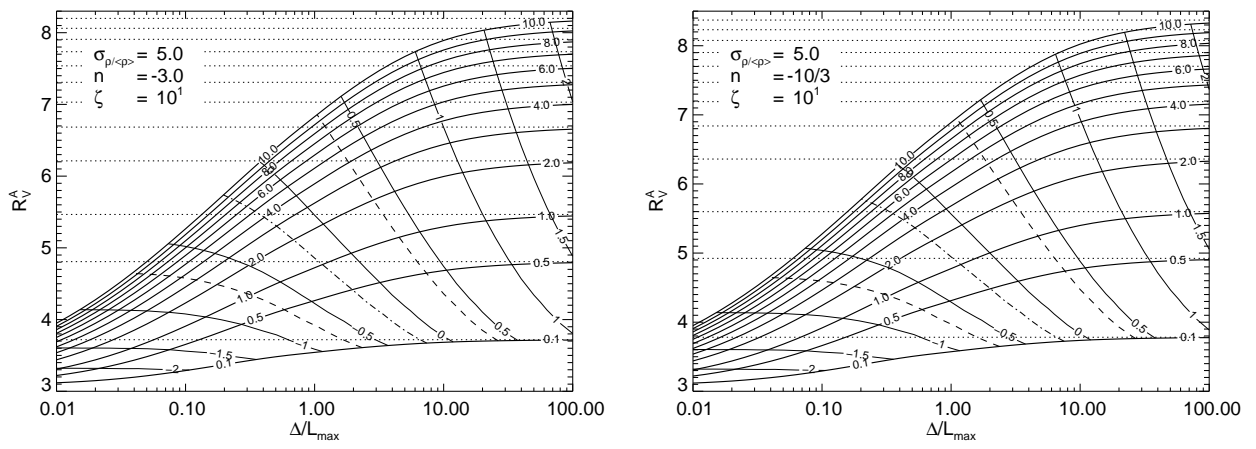


Fig. 16.— Same as the plots for $\sigma_{\rho/\langle\rho\rangle} = 5$ in Fig. 9 but assuming a power spectrum which extends only to $\zeta = 10$.